2015-12-01

Third Ventricle Width as a Metric for Fast and Efficient Detection of Atrophy in Traumatic Brain Injury

Christopher Scott Finuf
Brigham Young University - Provo

Third Ventricle Width as a Metric for Fast and Efficient Detection of Atrophy in Traumatic Brain Injury

Christopher Scott Finuf

A thesis submitted to the faculty of
Brigham Young University
in partial fulfillment of the requirements for the degree of

Master of Science in Neuroscience

Erin D. Bigler, Chair
Michael D. Brown
James D. Higley
Jonathan J. Wisco

Department of Physiology and Developmental Biology

Brigham Young University

December 2015

ABSTRACT

Third Ventricle Width as a Metric for Fast
and Efficient Detection of Atrophy in
Traumatic Brain Injury

Christopher Scott Finuf
Department of Physiology and Developmental Biology, BYU
Master of Science in Neuroscience

In an average year more than 1.7 million people will experience a traumatic brain injury (TBI) in the United States. It is known that atrophy occurs across a spectrum for TBI patients, ranging from mild to severe. Current conventional magnetic resonance imaging (MRI) methods are inconsistent in detecting this atrophy on the milder end of the spectrum. Also more contemporary imaging tools, although efficient, are too time consuming for clinical applicability. It is for these reasons that a quick and efficient measurement for detecting this atrophy is needed by clinicians. The measuring of third ventricle width had the potential to be this measurement, since it is known that ventricular dilation is an indirect measure of brain atrophy. This study used two different data sets acquired at multiple sites. A total of 152 TBI patients' MRI scans were analyzed with diagnosis ranging from mild to severe. They have been age matched with 97 orthopedic injury controls. All scans were analyzed using Freesurfer® auto-segmentation software to acquire cortical, subcortical, and ventricular volumes. These metrics were then used as a standard of efficacy which we tested the new third ventricle width protocol against. There was no statistically significant difference between the overall TBI group and OI group (Welch's $F(1,238.435) = 1.091$, $p= .267$). The complicated mild injury subgroup was significantly increased from the mild subgroup ($p= .001$, $d= .87$). The grand average third ventricle width measurement was the best prognosticator of all measures analyzed despite only predicting 35.1% of cases correctly. The findings suggest that the third ventricle width measurement is insensitive to atrophy between all groups as hypothesized.

Keywords: traumatic brain injury, traumatic axonal injury, third ventricle width

ACKNOWLEDGMENTS

I would like to express gratitude for the many people who have helped me with this project. I would like to acknowledge the faith, encouragement, and guidance of my mentor Dr. Erin D. Bigler who guided me to a project that was tailored specifically to my interests. He patiently directed me through this project and provided much needed encouragement on the long days. Tracy Abildskov provided the required technical assistance as well as an ample supply of refreshingly witty humor. To add to this, his unquenchable desire to help others even when faced with a workload of monumental proportions proved invaluable. Dr. Jo Ann Petrie instigated enlightening conversations on an array of topics which bolstered my sanity through the process. Also she, Dr. J. Dee Higley, and Dr. Dennis Eggett generously donated their time teaching me valuable statistical methods. Tyler Hammond and David Oleson helped greatly in data collection. They devoted long hours and kept positive attitudes throughout.

A special thanks to my family who have supported me physically, mentally, emotionally, spiritually, financially, grammatically, and every other way possible to get me to this point. They have always believed in me and this project is due in large part to their faith.

TABLE OF CONTENTS

LIST OF FIGURES

LIST OF TABLES

INTRODUCTION

Scope of Problem

In an average year more than 1.7 million people will experience a traumatic brain injury (TBI) in the United States (Bigler, 2008; Shenton et al., 2012). Currently, it is the leading cause of mortality and disability in young individuals in high-income countries (Maas, Stocchetti, & Bullock, 2008). Of reported cases, 15-25% are diagnosed as a moderate or severe TBI injury, while majority, between 75 to 85%, are characterized as mild in nature (Maas et al., 2008; Shenton et al., 2012). Clinically, severity of brain injury is commonly assessed using the Glasgow Coma Scale (GCS), a neurological testing measure (Bauer & Fritz, 2004). TBI severity is generally classified with severe injury level as 8 or less, moderate as 9-12, and mild as 13-15 (Bigler, Abildskov, et al., 2013; Y. B. Lee & Kwon, 2009). The moderate to severe TBI group manifests observable pathology such as shearing lesions, focal contusions, hematomas, and localized or diffuse swelling on conventional magnetic resonance imaging (MRI) sequences (Maas et al., 2008). In contrast, the mild TBI group typically has no identifiable abnormality on conventional MRI sequences (Bigler, 2008; Shenton et al., 2012). This is of particular significance because, of the mild TBI group, approximately 15-30% of patients manifest cognitive, physiological, and clinical symptoms that fail to resolve three months post-injury (Bigler, 2008; Shenton et al., 2012). The symptoms are variable amongst patients, but generally include dizziness, headache, irritability, fatigue, sleep disturbances, nausea, blurred vision, hypersensitivity to light and noise, depression, anxiety, as well as deficits in attention, concentration, memory, executive function, and speed of processing (Bigler, 2008; Shenton et al., 2012). This myriad of symptoms post-injury has been termed post-concussive syndrome (PCS), with patients exhibiting all or a mix of the above mentioned symptoms (Bigler, 2008).

This inconsistency in imaging modalities presents a challenge to the clinician seeking a diagnosis. Due to lack of understanding in injury progression and dearth of available treatments, this subset of the mild TBI group has been dubbed the "miserable minority" (Ruff, Camenzuli, & Mueller, 1996; Shenton et al., 2012). The pathophysiological mechanisms responsible for the manifestation and persistence of these symptoms have been the subject of a variety of research studies, but are still poorly known. Prior to advances associated with contemporary neuroimaging findings in mild TBI, it was believed that persistent maladaptive symptoms were a manifestation of a neurosis instead of anything related to neurological impairment, with many clinicians interpreting them exclusively within a psychogenic framework (Bigler, 2008). A prevailing theory today, however, is that they arise from neurological dysfunction. This neurological injury cannot consistently be detected by conventional MRI sequences, which are most often based on clinical judgement by just viewing the scan image but not applying any type of quantitative analysis (Edlow & Wu, 2012). Although more advanced post-processing imaging software and sequences have become available that are able to more reliably detect differences (Messina et al., 2011; Ostby et al., 2009; Ramasamy et al., 2009), they are limited in their clinical implementation primarily due to the time involved in performing their analyses and the extensive training required to become proficient using the software. It is for these reasons that a quick and efficient metric for detecting pathological differences, when present, in TBI patients of all severity types, using conventional imaging is needed. One of the most common observations of altered brain morphology following a brain injury is expansion of the ventricular system that occurs as a consequence of the loss of brain parenchyma. Since the ventricular systems is filled with cerebrospinal fluid (CSF), which is under pressure, there is an outward pressure gradient that results in ventricular expansion with the loss of brain tissue. Because of its central location

within the diencephalon the third ventricle might increase in size when damage has occurred potentially anywhere in the brain (Groswasser et al., 2002). Because of this, a linear third ventricle width (TVW) measurement could be this quick and efficient metric (Benedict et al., 2004; Nocentini et al., 2014; Sumowski, Wylie, Leavitt, Chiaravalloti, & DeLuca, 2013). Also, it has the potential to be a highly sensitive measure, since it is known that ventricular dilation is an indirect measure of global brain atrophy as well as an index of thalamic integrity (Bigler & Maxwell, 2012). It was the goal of this thesis to develop a linear TVW measurement to be able to distinguish between TBI patients with all levels of injury severity in MRI analyses.

General Overview of TBI Pathology

One of the many challenges of understanding TBI pathology progression in the brain is dealing with the heterogeneity of lesion types and locations (Bigler, Abildskov, et al., 2013). The location, type, and severity of these lesions are highly individualized amongst those that sustain a TBI (see Figure 1). For example, both individuals in Figure 1 sustained a TBI. The one on the left sustained a severe injury with massive structural damage as visualized on a MRI scan and the one of the right sustained a complicated mild injury with no visible abnormalities.

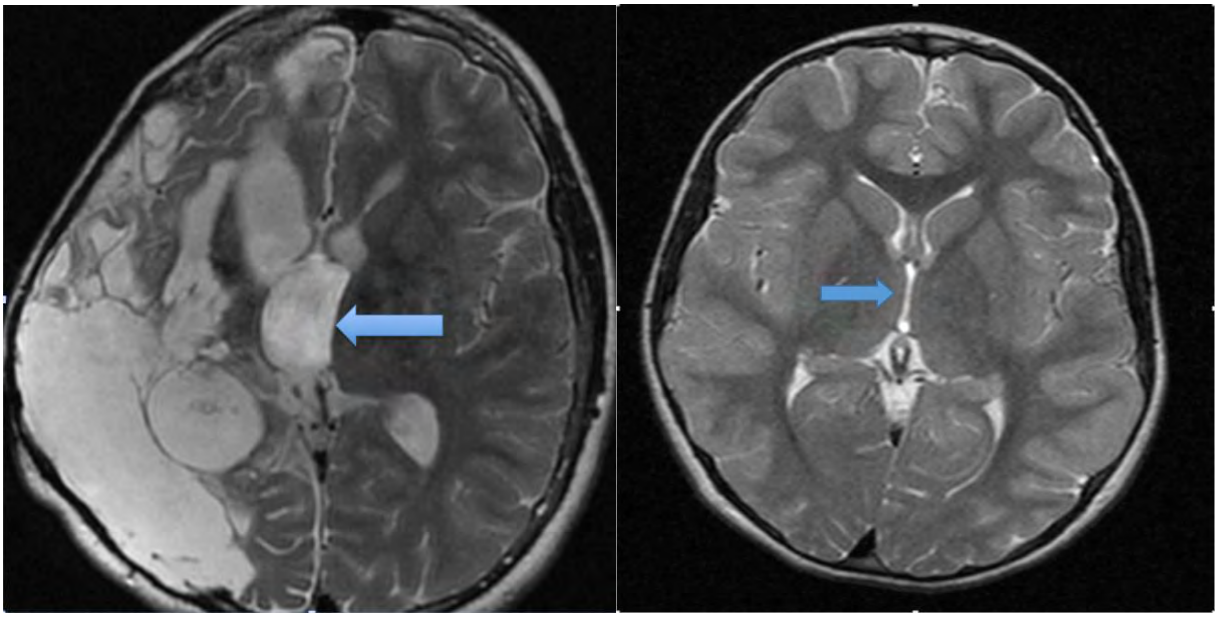

Figure 1: Severe vs. Mild TBI. Axial slice, a T2 MRI sequence, of a severe TBI (left). Right hemisphere ventricles are grossly dilated and significant encephalomalacia has occurred. Axial slice, a T2 MRI sequence, of a complicated mild traumatic brain injury (right). No pathology is visible. Also note the different sizes of the TVW on both images as highlighted by the blue arrows. TVW is average (right) and significantly dilated (left).

This heterogeneity is primarily due to the unique circumstances that surround each injury. These circumstances could include impact biomechanics, genetic, or experiential backgrounds (Bigler, Abildskov, et al., 2013). Age is another confounding variable. It has been documented that the thinner skull, open sutures, higher water content, progressing myelination, and higher sensitivity to oxidative stress of the pediatric brain can contribute to differences in injury and recovery patterns observed in children when compared to adults following TBI (Bauer & Fritz, 2004; Suskauer & Huisman, 2009). To control for age effects this thesis used datasets strictly comprised of pediatric patients.

In response to focal injury and destructive lesions, damaged neural tissue degenerates, leaving areas of reduced parenchymal volume within the region of injury. This damage is associated with a regional or focal increase of CSF, and often accompanied by residuals of the

original hemorrhagic contusion as by-products of degraded blood, referred to as hemosiderin (Bigler & Maxwell, 2012). In more focal injuries damage may leave regions of very focal pathology as in Figure 1, but the damage may also be non-specific and diffuse. Research has shown that white matter tracts are more vulnerable to injury in TBI because of their sensitivity to acceleration-deceleration, rotational, and shear and strain forces (Bigler, Abildskov, et al., 2013; McAllister et al., 2012). It is possible that white matter damage could be occurring at levels below the detection threshold of MRI technologies that would reveal a focal area of damage. For example, damage could be minor ranging from transient disturbance of transmembrane ionic homeostasis, to reversible disruption of axoplasmic transport via neurofilament and microtubule networks, to primary or secondary axotomy (Bigler & Maxwell, 2012; Edlow & Wu, 2012).

In the literature, any white matter degeneration and degraded myelin integrity is referred to as traumatic axonal injury (TAI) with the subset diffuse axonal injury (DAI), which occurs specific to shearing injuries to the white matter. To corroborate the idea that white matter damage is occurring below detection threshold of MRI technologies, histopathological investigations have confirmed that DAI may occur in mild traumatic brain injury (mTBI) patients (Blumbergs et al., 1994; Edlow & Wu, 2012). So despite MRI results being negative, post-mortem histopathological reports confirm the white matter damage is present in some mTBI patients who have died from non-neurological reasons and have gone to autopsy. Whether the damage is minor or not, the potential is present for there to be volume loss of brain parenchyma, meaning nonspecific damage may result in generalized loss of brain volume with correspondingly increased intracranial CSF.

Since the brain is under pressure in a vacuum, the ventricles expand to fill the space left unoccupied due to atrophy in focal or diffuse injuries, or the area back fills with CSF (See Figure

2). This condition, where there is an increase in CSF with no increase in pressure, is called hydrocephalus *ex vacuo* (Lemay & Hochberg, 1979; Sjaastad, Skalpe, & Engeset, 1969). In Figure 2, the image on the left depicts third ventricle dilation. The image on the right depicts lateral ventricle dilation as well as focal CSF back-filling in the frontal lobe. It has already been shown that ventricular dilation is a robust indirect measurement of brain atrophy (Booth et al., 2013; Sumowski et al., 2013). It was the aim of this thesis to assess whether third ventricle dilation would be sensitive enough to detect this diffuse damage reliably across different levels of injury severity. This is particularly important at the mild end of the TBI spectrum because differences are only inconsistently observed with current MRI technologies (Bigler, 2008; Shenton et al., 2012).

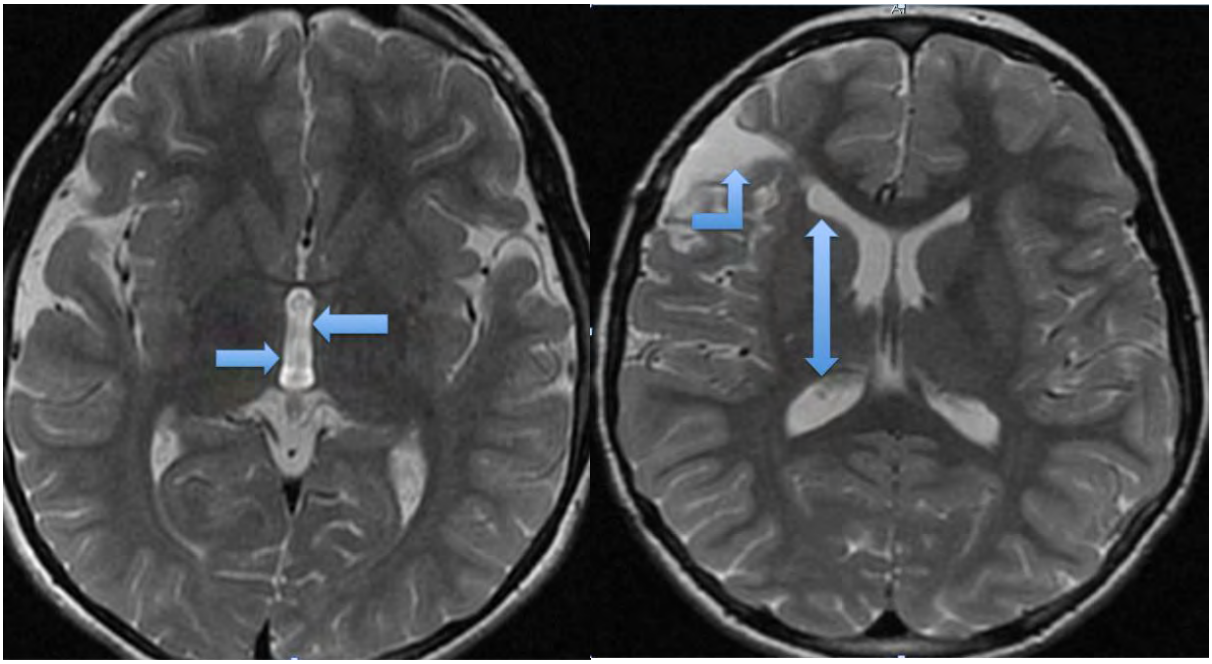

Figure 2: Ventricular Dilation. Axial slice, of T2 MRI sequence on left depicts TVW enlargement as shown by blue arrows. See Figure 1 for comparisons. Axial slice, of T2 MRI sequence on the right depicts dilation of the frontal horn of the lateral ventricle as well as CSF back filling of atrophied area in right frontal lobe shown by blue arrows.

MRI Correlates of TAI

Before the advent of MRI technologies, autopsy methods were the standard for measuring brain volumes and ascertaining pathology (Blatter et al., 1997). As technology progressed, it was shown that MRI techniques were particularly accurate at measuring atrophic changes in vivo (Blatter et al., 1997). This provided researchers with the opportunity to follow pathological changes in longitudinal studies, which was not possible with autopsy methods.

MRI sequences are able to distinguish a gamut of signal abnormalities. These abnormalities range from white matter hyperintensites (WMH) to deposits of blood by-products, also known as hemosiderin. These WMH's are thought to represent degraded myelin integrity suggestive of Wallerian degeneration and thought to be a marker of TAI and DAI (Bigler, Abildskov, et al., 2013; Zhan et al., 2009). In addition to this, it has been suggested that they could reflect other mechanisms, such as apoptosis, inflammation, excitotoxicitity, or prolonged hypoperfusion (Sidaros et al., 2009). In moderate to severe TBI, WMHs are more common, while in mTBI they are infrequent. In Figure 3 below, the image on the left is a severe TBI patient with multiple regions where WMHs are evident, with the largest highlighted by the blue arrows. However the mTBI patient on the right displays no such damage.

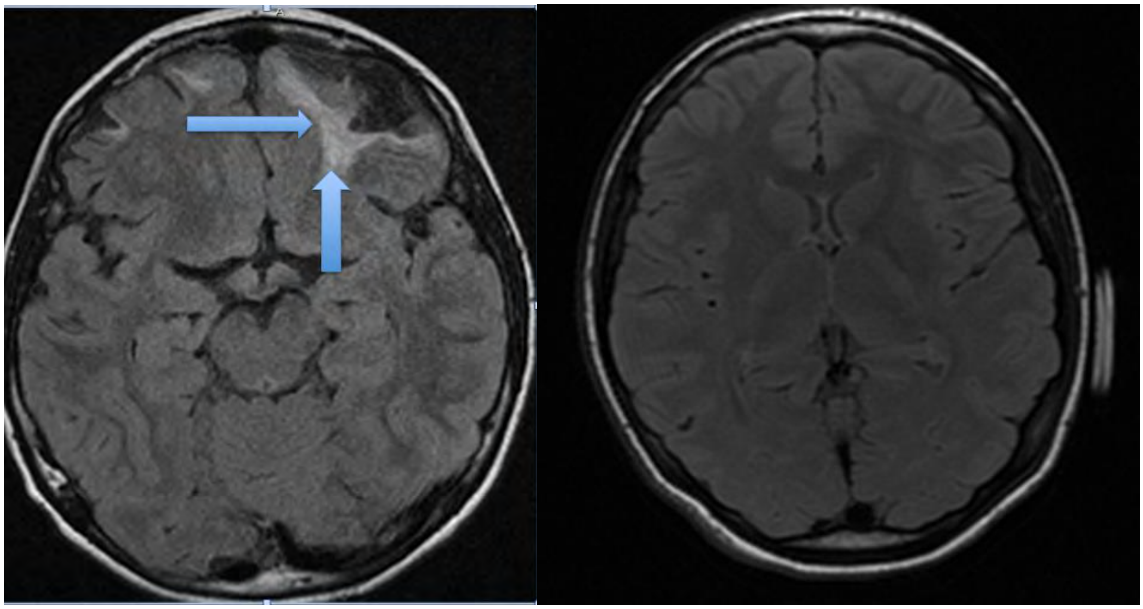

Figure 3: White Matter Hyperintensities. Axial slice, on a FLAIR sequence (left) is showing a large WMH in left frontal lobe of a severe TBI patient. The FLAIR sequence has been shown to have greater efficiency at detecting WMH. Axial slice, on a FLAIR sequence (right) shows no visible pathology in an mTBI patient.

WMHs are especially detected by certain MRI sequences like the fluid attenuated inversion recovery (FLAIR) sequence (Bigler, Abildskov, et al., 2013). Significant attention has been directed toward the development of advanced neuroimaging sequences and post-processing techniques for the detection of DAI. Susceptibility weighted imaging (SWI), diffusion tensor imaging (DTI), diffusion weighted imaging (DWI), and (1)H magnetic resonance spectroscopy are among some of the sequences that have been developed, with DTI showing to be particularly sensitive to DAI (Suskauer & Huisman, 2009). As an aid to image processing multiple post-processing software techniques have become available including- Freesurfer®, FSL, SPM, and ANALYZE® (Fischl, 2012; Friston, Frith, Liddle, & Frackowiak, 1991; Robb et al., 1989; Smith et al., 2004). While these techniques are being used, because post-processing can take exorbitant amounts of time, they have not found their way into clinical implementation (Edlow & Wu, 2012; Unger et al., 2010).

As technology progresses, major challenges face clinicians on how to implement these advanced imaging techniques and research developments for the maximum benefit of their patients. As with all innovative technology, there are numerous methodological factors that must be considered for accurate interpretation. Also for some techniques, the data acquisition and post-processing time may limit the feasibility of clinical implementation (Edlow & Wu, 2012). The goal of this study was to bridge this gap by potentially bringing these advances to the clinician in a unique way. To accomplish this the current thesis developed and implemented a simple linear TVW measurement with the aim that it would be a quick and efficient method comparable in sensitivity to diffuse atrophy as current labor intensive volumetric measurements acquired using Freesurfer® post-processing software. The main advantages of this protocol was eliminating the need for complicated post-processing software and providing the clinician with a diffuse atrophy sensitive metric using just conventional imaging methods. Most importantly not all clinical MRI studies involve research quality scans and imaging sequences, which would preclude any kind of sophisticated image analysis. If a simple measure of TVW can detect atrophic changes, this may provide the clinician with a quick measure of brain integrity.

Third Ventricle Anatomy and Physiology

The ventricular system has been the focus of multiple studies, and its width and volume have been used as indirect measures of brain atrophy in a variety of disorders (Ambarki et al., 2010; Kempton, Stahl, Williams, & DeLisi, 2010; Maria Alvarez et al., 2011; Pitel, Chanraud, Sullivan, & Pfefferbaum, 2010). Although the naming of individual ventricular structures has changed throughout the course of history, it is commonly acknowledged today that the ventricular system consists of four freely communicating CSF filled cavities: the two lateral ventricles, the third ventricle, and the fourth ventricle (Mortazavi et al., 2014; Schiller, 1997).

This system is believed to function chemically as a waste removal system and mechanically as a water jacket for the brain and spinal cord serving as support, lubricant, and buffer (Calmon & Roberts, 2000).

The third ventricle communicates with the lateral ventricles through the interventricular foramen on its anterosuperior aspect and the cerebral aqueduct of Slyvius on its posteroinferior aspect (Mortazavi et al., 2014). Since the third ventricle is a cavity filled with CSF, it is important to note the structures that form the roof, walls, and floor of its enclosure. The roof is composed of four layers: the uppermost layer is formed by the body of the fornix anteriorly and the crura and hippocampal commissure posteriorly (Mortazavi et al., 2014). Below this are two membranous layers of tela choroidia with a thin sheet of blood vessels running in between (Mortazavi et al., 2014). The anterior wall is composed of the following structures superior to inferior: diverging columns of the fornix, foramina of Monro, anterior commissure, lamina terminalis, optic recess, and the optic chiasm (Mortazavi et al., 2014). The floor is composed as follows, anterior to posterior: optic chiasm, optic recess, the infundibulum of the hypothalamus, the tuber cinereum, mammillary bodies, and the tegmentum of the midbrain (Mortazavi et al., 2014). The posterior wall starts, inferior to superior, with the aqueduct of Sylvius, the posterior commissure, the pineal body and its recess, the habenular commissure, and the suprapineal recess (Mortazavi et al., 2014). Lastly, the upper of the lateral walls is composed of the medial surface of the anterior two-thirds of the thalamus. The lower part is composed of the hypothalamus anteriorly and the subthalamus posteriorly (Mortazavi et al., 2014).

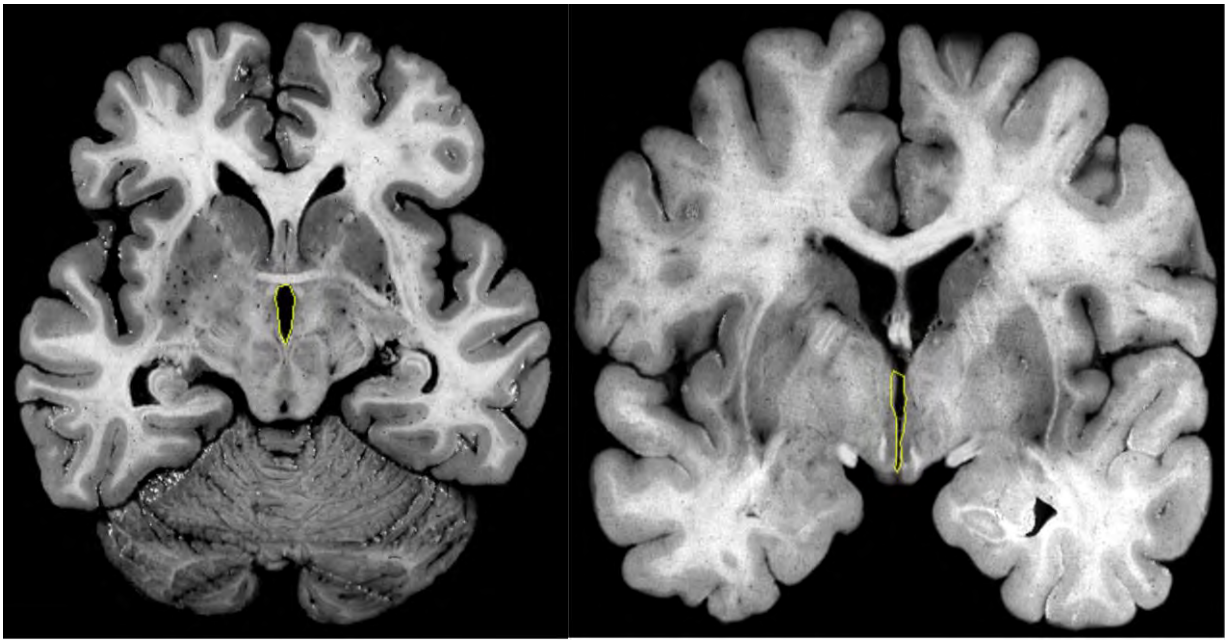

Figure 4: Third Ventricle Anatomy. Axial section (left) and coronal section (right), depict the third ventricle at the level of the anterior commissure. Third ventricle is outlined in yellow on both images. Used with permission from: Digital Anatomist Project at the University of Washington. Washington Brain Atlas: http://www9.biostr.washington.edu:80/cgi-bin/DA/PageMaster?atlas:Neuroanatomy+ffpathIndex/Horizontal^Forebrain/Anterior^Commissure+2 and http://www9.biostr.washington.edu:80/cgi-bin/DA/PageMaster?atlas:Neuroanatomy+ffpathIndex/Coronal^Forebrain/Anterior^Commissure+2

It has been postulated that due to the strategic location of the third ventricle, being encompassed by thalamic and limbic structures, that third ventricle *ex vacuo* dilation is indicative of thalamic atrophy. (Sumowski et al., 2013; Tiemann, Penner, Haupts, Schlegel, & Calabrese, 2009). Conversely, multiple studies have shown a decrease in exclusively cortical gray matter to be inversely related to third ventricle volume (Cannon et al., 2015; Dabbs et al., 2012; J. H. Lee et al., 2013; Yang et al., 2012). Merging these findings, this thesis suggests that a linear TVW measurement does not exclusively measure subcortical atrophy but is a global measure of brain atrophy independent of lesion location or size. This could potentially be due in part to the fact the thalamus is particularly sensitive to shear and strain injury due to the long axons of the corticospinal tract (see Figure 5) and thalamic nuclei that send diffuse and specific efferent

projections connecting cortical, cerebellar, and subcortical regions (Little et al., 2010; Wakana, Jiang, Nagae-Poetscher, van Zijl, & Mori, 2004). Damaging one could invariably damage the others.

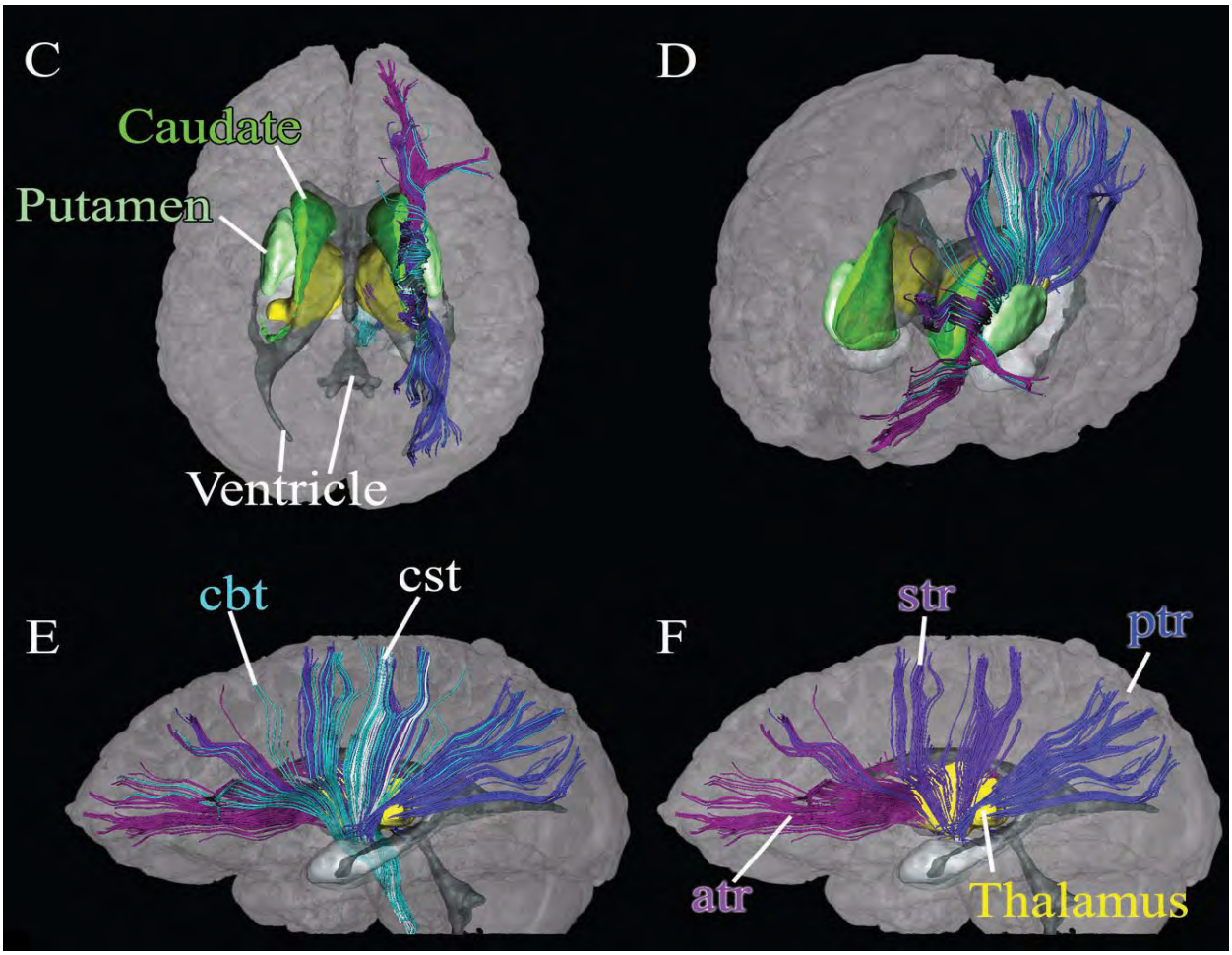

Figure 5: Thalamic Projections. The corticospinal tract (cst) in white, anterior thalamic radiation (atr), superior thalamic radiation (str), and posterior thalamic radiation (ptr) are shown in C-F. As illustrated, thalamic fibers are distributed throughout the cortex superior and inferior to the thalamus which makes it a potentially good measure of global atrophy. Used with the permission of the Radiological Society of North America (RSNA). Figures 2, 3 of Wakana S, Jiang H, Nagae-Poetscher L M, et al. Fiber Tract–based Atlas of Human White Matter Anatomy. Radiology 2004;230:77-87.

Linear Third Ventricle Width Measurement Studies

In vivo linear TVW measurements date back to the 1950's, when pneumoencephalograms were employed to measure the TVW in Parkinson's disease patients (Gath, Jorgensen, Sjaastad, & Berstad, 1975). Pneumoencephalograms were obtained invasively and necessitate a CSF/air transfusion through a spinal tap to increase contrast on x-ray scans of the brain. No significant correlation was found between the degree of central atrophy (third ventricle width) and severity of clinical symptoms (Gath et al., 1975). This lack of correlation potentially could have been due to the poor image quality acquired by pneumoencephalograms during that time period.

Concurrently during the early 1970's computed tomography (CT) was developed and clinically implemented. CT scanning became an industry standard and remains so in acute head injuries. A common method for measuring the TVW on CT scans was standardized (Kaplan, Lazoff, Kelly, Lukin, & Garver, 1990). To start, TVW measurements were made on those sections displaying maximum body of the third ventricle based on visual instruction (Kaplan et al., 1990). These were measured on magnified images using a dissecting microscope with a calibrated ocular (Kaplan et al., 1990). A transparent ruler was the tool of measurement on hard copy images (Groswasser et al., 2002; Reider et al., 2002) because there were no computer based methods for linear measurements.

It was in CT studies that TVW measurements started showing potential as a sensitive brain atrophy measurement. One study, which examined the effects of traumatic brain injury in military personal who served in Vietnam, found significant correlation between TVW and multiple cognitive neuropsychological assessments (Groswasser et al., 2002). Similar results were found in a multiple sclerosis study as well (Rao et al., 1985). In addition to these studies,

another study looked at TVW in schizophrenia and found that an increased TVW correlated with decreased ANS arousal and negative symptom schizophrenia (Dykes, Mednick, Machon, Praestholm, & Parnas, 1992).

Over the next decade, a new superior imaging modality started gaining relevance. MRI, which uses magnetic fields instead of X-rays, produces a superior image to CT and better differentiation between dense and soft tissues. This allowed for more accurate measurements of the third ventricle when combined with computational methods. A common MRI measuring protocol used today in acquiring TVW is to draw a line first through the long axis of the third ventricle, parallel to the interhemispheric fissure in the FLAIR axial section where the third ventricle was most visible (Benedict et al., 2006; Benedict et al., 2004). The width is then measured by drawing a second line perpendicular to the first at its midpoint (Benedict et al., 2006; Benedict et al., 2004). This TVW measurement has become the standard in multiple sclerosis research, proving to be highly robust as an indirect measure of brain atrophy (Booth et al., 2013; Sumowski et al., 2013). Other methods have been utilized to study a variety of neuropsychological ailments, such as bipolar disorder (Cousins et al., 2010), Alzheimer's disease (Rodriguez et al., 2012), and Parkinson's disease (Gross et al., 1999; Obwegeser et al., 2000). All of these studies used different TVW measurement protocols that appear to be effective in their own right. To the best of my knowledge, no MRI TBI studies have used linear TVW measurements.

One of the purposes of this thesis was to fill this gap. In order for measurements to become adopted and standardized in the scientific community it has to show robustness and comparability to current standards of the day. Currently, complicated post-processing software using volumetric measurements, not linear, are utilized to measure brain atrophy in MRI TBI

studies. These processes are not only laborious and protracted in getting results but are incompatible with many types of TBI lesions. Referring back to Figure 1, axial slice (left) shows severe and diffuse abnormalities that a complicated post-processing software, such as Freesurfer®, is unable to process. The new TVW protocol developed here is impervious to such limitations. It is quicker and independent of lesion types compared to Freesurfer®. This protocol is followed simply by visually inspecting scans for a slice that has a continuous view of the third ventricle and no part of the midbrain in visible. This slice should correspond to a view of the third ventricle just below the interthalamic adhesion. On this slice a line region of interest (ROI) will be drawn through the long axis of the third ventricle parallel with the interhemispheric fissure and three perpendicular measurements at 10, 50, and 90% of that ROI will be taken as seen in Figure 7. A more detailed protocol is discussed in the methods section and Appendix A.

FreeSurfer® Auto Segmentation Software Background

Freesurfer® (http://surfer.nmr.mgh.harvard.edu/) is the prototype automated post-processing software available to date (Fischl, 2012). Today Freesurfer® is able to do multiple analyses such as take volumetric segmentation of most macroscopically visible brain structures, segmentation of hippocampal subfields, inter-subject alignment based on cortical folding patterns and segmentation of white matter fascicles using diffusion MRI. In addition to this, it can parcel cortical folding patterns, estimate architectonic boundaries from in vivo data, map thickness of cortical gray matter, and construct surface models of the human cerebral cortex (Fischl, 2012). Freesurfer® has become a staple in MRI analysis research, and multiple studies have utilized its tools of analysis to elucidate the structural, functional, and connectivity of the human brain (Messina et al., 2011; Ostby et al., 2009; Ramasamy et al., 2009).

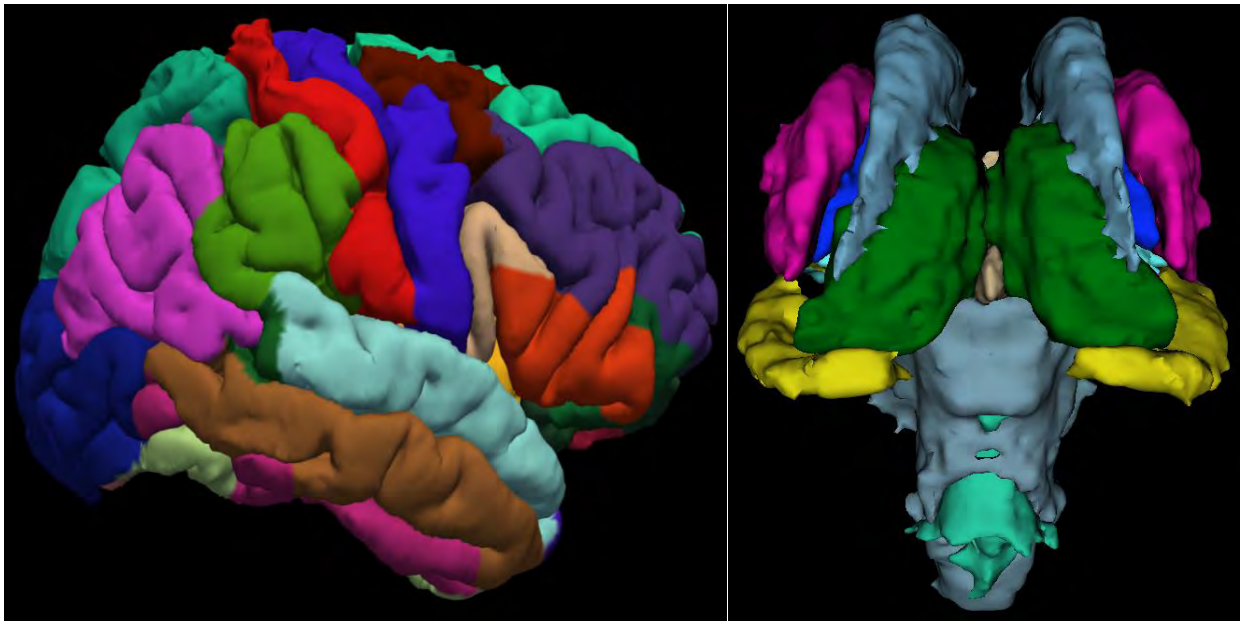

Figure 6: Freesurfer® Segmentation. The image on the left shows Freesurfer® cortical segmentation of the author's brain. The image on the right depicts sub-cortical segmentation. With this software, one is able to acquire volumes of cortical and subcortical areas with relative accuracy.

Operator controlled image quantification (manual tracings) was the standard of volumetric analysis before the advent of auto-segmentation software (Jovicich et al., 2009; Messina et al., 2011). Just like manual tracings on MRI images have been shown to be comparable to autopsy reports (Blatter et al., 1997), so has Freesurfer® auto-segmentation values been shown to be comparable to manual tracings on MRI images (Bigler et al., 2010; Jovicich et al., 2009; Messina et al., 2011).

Some drawbacks to Freesurfer® include post-processing times. Multiple hours, large computing requirements using batch processes on a supercomputer, and extensive training on how to use the program are necessary (Sanchez-Benavides et al., 2010). Also it is fraught with classification problems if movement or artifact are present. So although Freesurfer® is an integral part of research it is not the most efficient for clinical implementation at this time.

Rationale for the Study

It was clear from the literature that TVW measurements were not only being used but were shown to be effective and robust indirect brain atrophy measurements for a variety of neurological conditions. Surprisingly, there was no established TVW measurement being used in MRI TBI research. Seeing a gap in utility and a clinical need for a metric with quick and reliable detection of atrophy in mTBI patients, a TVW protocol was created. One that was believed to be an improvement upon other TVW protocols in other fields. This protocol was measured against the current standard of MRI analysis, which is volumetric measurements derived from Freesurfer® post-processing software.

Also, the relevance of demonstrating that a TVW measurement is as robust as the Freesurfer® volumetric outputs means that clinicians would get pertinent information about their patients in a timely manner regardless of injury. This is because MRI scans rendered incompatible with Freesurfer® software due to significant artifact can still be included in TVW analyses.

Hypothesis

It was hypothesized that the TVW measurement protocol, specifically the grand average TVW measurement would be significantly larger in the overall TBI injury group compared to orthopedic controls. Specifically, that TBI patients at each level of severity will have larger TVW compared to the one preceding it in severity. Also that grand average TVW measurement will predict injury severity between all subgroups. Lastly, that the grand average TVW measurement will be highly correlated and comparable to Freesurfer® derived volumes in injury group predictability.

METHODS

Participants/Diagnosis

Social Outcomes in Brain Injury in Kids (SOBIK) . All participants were recruited and scanned during a 4 year period (2006-2010) as part of a multisite (Toronto, Canada, Columbus, Ohio, and Cleveland, Ohio) study of social outcomes in children with TBI. This study was conducted in accordance with established ethical guidelines and received institutional ethics approval for all three neuroimaging sites. Also, all participants provided written informed consent/assent prior to participation.

A total of 143 participants were recruited with 124 undergoing MRI scanning at a minimum of 6 months post-injury. 5 patients were excluded due to poor scan quality such as to prevent analysis. Patient's age ranged between 5-13 years of age. The TBI group was composed of 82 children who experienced TBIs ranging from complicated mild to severe. Inclusion criteria required hospitalization and those who had a reported day-of-injury (DOI) post resuscitation GCS score of 12 or less, or GCS score of 13-15 with positive imaging results for skull fracture or brain insult on CT scans. TBI severity was determined by GCS score, with severe injury level classified as 8 or less, moderate as 9-12, and complicated mild as 13-15. The presence of a skull fracture, some form of acute intracranial hemorrhage, or identifiable edema on computed tomography (CT) was required in concurrence with GCS score greater than 12 to meet inclusion criteria for the complicated mild TBI group (Bigler, Abildskov, et al., 2013). CT findings of these patients have been summarized and published earlier (Dennis et al., 2012).

The control group was composed of 61 children who had some type of orthopedic injury (OI). The GCS score was still recorded as 15 despite no diagnosis of TBI or facial fractures or any other indication of possible head injury in the control group.

University of California at San Diego (UCSD) .This study is still in progress. Its study design goals are to enroll 220 children between ages 8-15 who are consecutively seen for mTBI and 110 children seen consecutively for orthopedic injuries at the Emergency Department of Rady Children's Hospital. These children have undergone or will undergo an MRI at 6 months post-injury. This study was conducted in accordance with established ethical guidelines and received institutional ethics approval. Also, all participants provided written informed consent/assent prior to participation.

The mTBI group includes children who have suffered a closed head injury that resulted in an observed loss of consciousness, a Glasgow Coma Scale (GCS) score of 13 or 14, or at least two symptoms of concussion as noted by the Emergency Room medical staff (i.e., persistent post-traumatic amnesia, transient neurological deficits, vomiting, nausea, headache, diplopia, dizziness).

Exclusion criteria includes those with delayed neurological deterioration, loss of consciousness greater than 30 minutes or had a GCS score of less than 13. Other exclusion criteria for the mTBI group include the following: 1) associated injury that is severe, documented with the Abbreviated Injury Scale (AIS) score greater than 3; 2) associated injury that is likely to interfere with cognitive testing (e.g., injury to dominant upper limb); 3) hypoxia, hypotension, or shock associated with the injury; 4) alcohol or drug ingestion involved with the injury; 5) documented history of previous TBI meeting the above criteria; 6) pre-injury neurological disorder, schizophrenia, pervasive developmental disorder, or mental retardation; 7) any medical

contraindication to MRI; 8) any injury requiring neurosurgical intervention; or 9) illegal immigrant status.

Inclusion criteria for children with orthopedic injuries will be the presence of upper or lower limb fractures associated with AIS scores of 3 or less. Exclusion criteria for the OI group include: 1) injury to the head or TBI; 2) associated injury that is severe, documented with the Abbreviated Injury Scale (AIS) score greater than 3; 3) associated injury that is likely to interfere with cognitive testing (e.g., injury to dominant upper limb); 4) alcohol or drug ingestion involved with the injury; 5) documented history of previous TBI meeting the above criteria; 6) pre-injury neurological disorder, schizophrenia, pervasive developmental disorder, or mental retardation; 7) any medical contraindication to MRI; or 8) illegal immigrant status.

Table 1: Participants Information

Data Sets	OI	Mild TBI	Complicated mild TBI	Moderate TBI	Severe TBI	Total
Social Outcomes in Brain Injury in Kids	51	0	37	11	20	119
University of California in San Diego	46	84	0	0	0	130
Total	97	84	37	11	20	249

MRI Data Acquisition and Analysis

Social Outcomes in Brain Injury in Kids (SOBIK). MRI was performed during the chronic phase of injury (minimum = 6 months post injury; average = 2.7 years post trauma), when lesion type and location have stabilized (Blatter et al., 1997; Ross, 2011). The Toronto and Columbus sites used GE Signa Excite scanners and the Cleveland site used a Siemens Symphony scanner but all studies used a magnetic strength of 1.5 T. All sites acquired the following sequences on each participant: thin slice, volume acquisition T1-weighted ultrafast 3-dimensional gradient echo, a dual-echo proton density (PD)/T2-weighted sequence; FLAIR; and GRE. Identical phantom imaging was performed at the beginning to check the uniformity of image acquisition and image quality across the multiple sites (Bigler, Abildskov, et al., 2013).

University of California at San Diego (UCSD). MRI was performed using a GE Discovery 3T scanner. The following sequences on each participant were acquired: FLAIR, T1 structural, DTI, and SWI.

Image Analysis

Third ventricle width measurements were performed following the new protocol described below and in Appendix A. Cortical, subcortical volumes, and total brain volumes (TBV) were acquired using the auto-segmentation software, Freesurfer® version 5.3.0 on the Mary Lou Fulton Supercomputer at Brigham Young University.

Third Ventricle Width Measurement Protocol

Third ventricle width measurements were acquired using axial PD-T2 TSE sequences in the SOBIK dataset and FLAIR sequences in the UCSD dataset. Osirix program v5.7.1

measurement tools were utilized. 3 total measurements were taken. Simplified step by step instructions are as follows: *1.* Start ventral and move dorsally slice by slice until a continuous view of the third ventricle is visible and no part of the midbrain in visible. This slice should correspond to a view just below the interthalamic adhesion. *2.* On this slice, a line region of interest (ROI) will be drawn through the long axis of the third ventricle parallel with the interhemispheric fissure. *3.* Three perpendicular measurements at 10, 50, and 90% of the line previously drawn on this slice will be taken and recorded. Some exceptions do apply. For a detailed explanation see Appendix A and Figure 7.

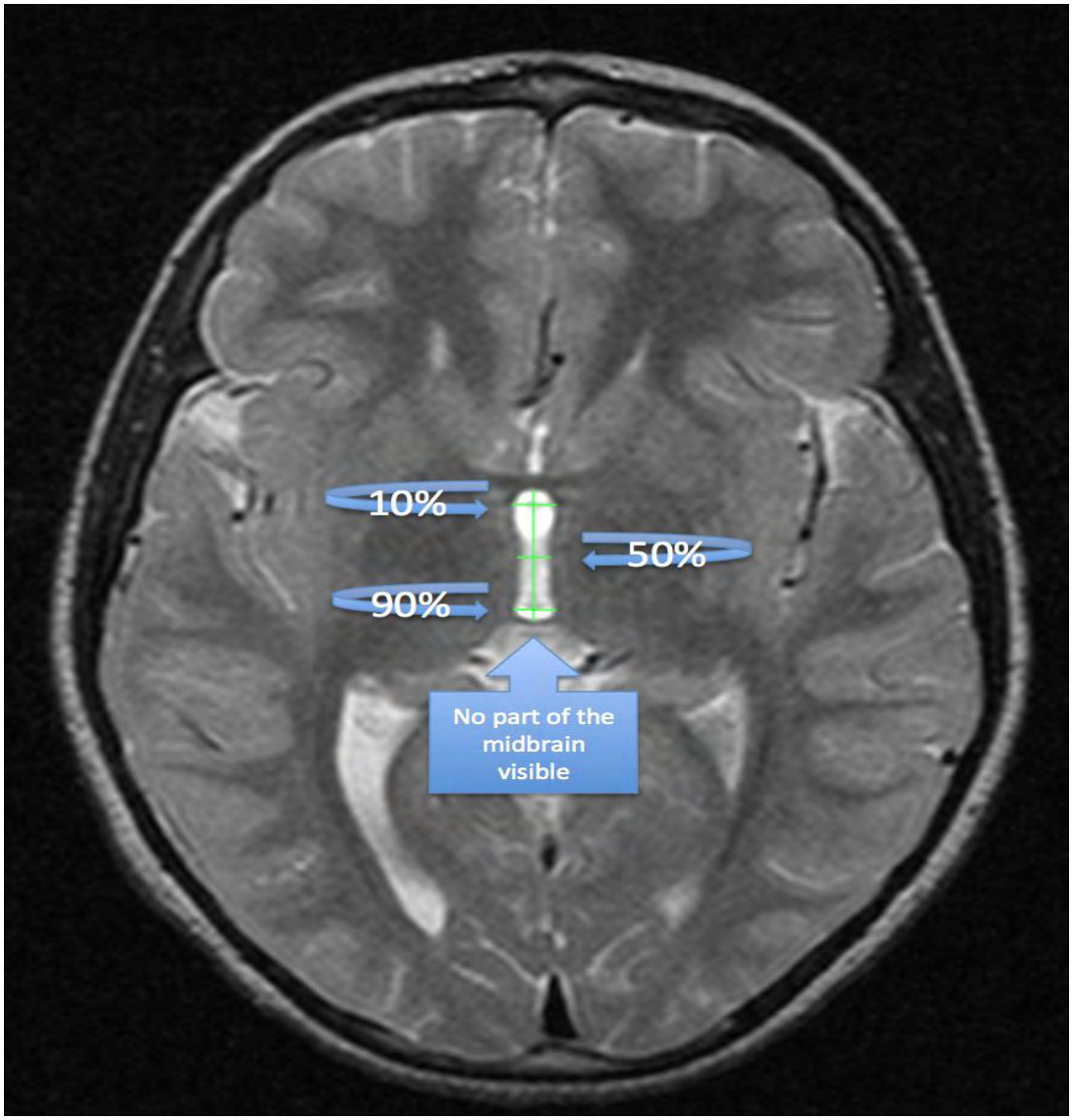

Figure 7: TVW Protocol. Three individual linear measurements at 10, 50, and 90% of vertical line on an axial T2 MRI image. These are taken as described in step 2 of the protocol described above. Measurements are shown by green lines.

Test-retest Reproducibility

Variability is inherent with manual protocols. To ensure reliability of linear measurements, all MRI scans were analyzed by two raters, DO and TH. Intra-rater reliabilities were obtained by having both raters apply the TVW protocol twice to the first ten scans in each data set. A Cronbach's alpha reliability test was used to ensure a high intra-rater agreement ($\alpha \geq$

.84). Inter-rater reliabilities were then calculated for each of the three measurements using the Cronbach's alpha reliability test again to ensure a high inter-rater agreement ($\alpha \geq .90$). Each of the three measurements were averaged separately and together to yield 4 total measurements per subject. These averages were used in the statistical analyses.

Statistical Analysis

Analysis of data was carried out using SPSS statistical software (version 23.0, SPSS Inc. Chicago, IL). A Welch's t-test was run with all TBI patients in one group compared against OI controls. Total brain segmentation volume was controlled for by normalizing all values as a ratio to total brain segmentation volume (Filbey, McQueeny, Kadamangudi, Bice, & Ketcherside, 2015). An ANCOVA was run with age at testing and total brain segmentation volume as covariates to discover potential significant differences between all subgroups (Takeuchi et al., 2015). A post-hoc test with a Bonferroni correction was run in conjunction with the ANCOVA. To assess between measurement correlations a Spearman's rank order correlation test was run using the grand average TVW measurement, 3rd ventricle volume, left thalamus volume, right thalamus volume, and total brain segmentation volume. Effect sizes, as measured with Cohen's d, were manually calculated. To determine prognosticating power a discriminant function analysis was run on each individual measure while discriminating between injury groups.

RESULTS

Demographic data is presented in Table 2. Controls were statistically significantly younger at time of testing than the TBI group and although total brain segmentation volume was not statistically different between groups there was a statistically significant difference between sexes; therefore in subsequent analyses, total brain segmentation volume were statistically controlled for in two different ways. First, by having all volumes normalized as ratios of total brain segmentation volume (Filbey et al., 2015), and second as ANCOVA covariates (Takeuchi et al., 2015). Age at testing was only controlled for as an ANCOVA covariate. One patient was removed from all statistical analyses *a priori* due to it being an extreme outlier.

Table 2: Demographics for Traumatic Brain Injury (TBI) and Orthopedically Injured (OI) Participants

Characteristic	TBI	OI	t -Values
No. of subjects	152	97	
Female	57	31	
Male	95	66	
Age at Testing (y)			
Mean (SD)	11.61 (2.12)	11.01 (1.90)	t(246)= -2.345, p= 0.020
Range	7.64-15.75	8.16-15.28	
WASI-IQ			
Mean (SD)	103.53 (14.54)	103.79 (15.41)	t(246)= .044, p= 0.965
Range	69-135	45-139	
BrainSegVol (cm^3)			
Mean (SD)	1196.60 (104.45)	1209.82 (113.00)	t(246)= .928, p= 0.354
Range	898.65-1489.94	872.84-1551.29	
Characteristic	Female	Male	t-Values
BrainSegVol (cm^3)			
Mean (SD)	1136.83 (107.16)	1237.23 (91.39)	t(246)= -7.797 p≤ 0.0009
Range	872.84-1551.29	1045.53-1498.31	

Note: BrainSegVol= Total Brain Segmentation Volume, WASI-IQ= Wechsler Abbreviated Scale of Intelligence-Intelligence Quotient, y= years

Inter-Rater and Intra-Rater Reliability

The protocol had a high level of inter-rater and intra-rater consistency as assessed by Cronbach's alpha. Results are displayed in Table 3 below.

Table 3: Inter-rater and Intra-rater Reliability Scores as Assessed by Cronbach's Alpha in the Social Outcomes in Brain Injury in Kids (SOBIK) and University of California at San Diego (UCSD) Data Sets

	Inter-rater		Intra-rater	
Data Set	SOBIK	UCSD	SOBIK	UCSD
Measurement	α		α	
10%	.948	.910	.887	.971
50%	.969	.903	.864	.985
90%	.954	.912	.961	.845
GA	.976	.913	.962	.842

Note: α= Cronbach's alpha, 10% = 10% width measurement, 50% = 50% width measurement, 90% = 90% width measurement, GA = grand average of all three measurements

Hypothesis 1: The Overall TBI Group Will Have Larger Grand Average TVW Compared to Orthopedic Injury Controls.

The assumption of homogeneity of variances was violated as assessed by Levene's test ($p= .044$), so a Welch's t-test was run instead of the ANCOVA. Total brain volume was controlled by normalizing all values as a ratio to total brain segmentation volume (Filbey et al., 2015). Standardized residuals for individual groups and the overall model were not normally distributed, as assessed by a Shapiro-Wilk test ($p\leq 0.0009$). Both groups had a slight positive skew. Despite this, since one-way ANOVA is known to be fairly robust against deviations from normality, especially when groups are skewed in similar ways (Sawilowsky & Blair, 1992), it was the preferred statistical procedure. There were 3 outliers in the dataset as assessed by cases of standardized residuals greater than ±3 standard deviations. The one-way ANOVA was run with and without the outliers and statistically significant results were unchanged. The grand average TVW measurement as a ratio to total brain segmentation volume was not statistically

significantly different between TBI and OI groups, [Welch's F(1,238.435) = 1.091, p= .267; see Table 4 and Figure 8].

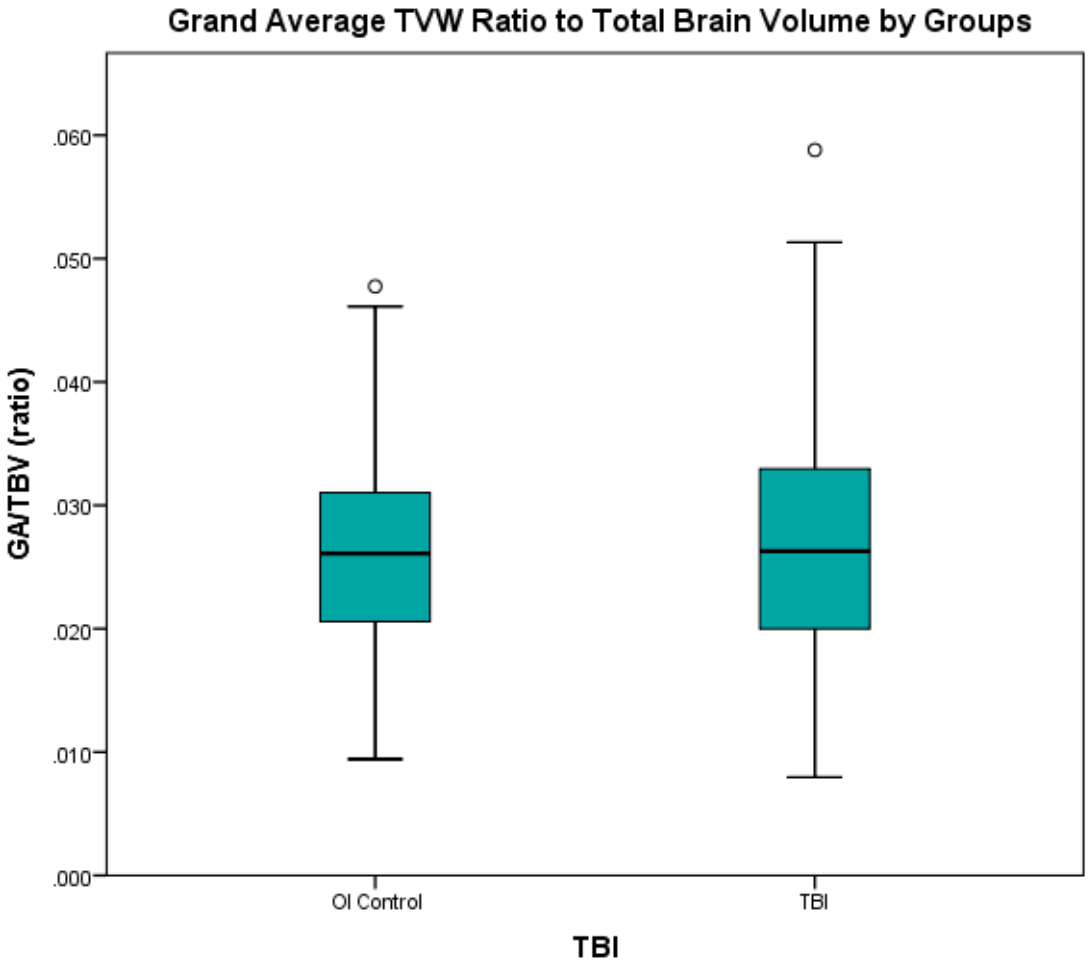

Figure 8: TBI vs. OI Control. Boxplot showing between group differences for the grand average TVW measurement as ratio to total brain segmentation volume (GA/TBV). Center line is group median and bars represent 95% confidence intervals. There were no statistically significant difference between TBI and OI groups (p= .267). Outliers represent data points approximately 1.5 standard deviations from the edge of the box according to SPSS Statistics.

Table 4: Adjusted and Unadjusted Means and Variability for the Overall Average Third Ventricle Width Measurement as a Ratio of Total Brain Volume

		Unadjusted		Adjusted	
	N	M	SD	M	SE
TBI	151	3.281	1.234	3.317	.093
Control	97	3.181	1.048	3.125	.117

Note: N = number of patients, M = Mean, SD = Standard deviation, SE = Standard error. All third ventricle width metrics measured in millimeters (mm). Control group is orthopedically injured patients.

Hypothesis 2: TBI Patients at Each Level of Severity Will Have Larger Grand Average TVW Compared to the One Preceding It in Severity.

There was a linear relationship between the grand average TVW measurement, and covariates, age at testing and total brain segmentation volume, as assessed by visual inspection of a scatterplot. Homogeneity of regression slopes was confirmed as both interaction terms, ageattesting*injurygroup and brainsegvol*injurygroup, were not statistically significant, [$F(4,233) = .586$, $p= .673$, $F(4,233) = .494$, $p= .740$, respectively]. There was homogeneity of variances as assessed Levene's test for homogeneity of variances ($p= .103$). Standardized residuals of the dependent variable did not meet the assumption of normality between all groups however as assessed with a Shapiro-Wilk test. Moderate and complicated mild groups had $p> .05$ while the severe, mild and control groups had p-values equal to .029, .002 .003, respectively. All had a slight positive skew. The normality of standardized residuals for the overall model also did not meet this assumption, being also positively skewed, as assessed with a Shapiro-Wilk test, $p\leq 0.0009$. Despite this, since ANCOVA is known to be fairly robust against deviations from normality, especially when groups are skewed in similar ways (Sawilowsky & Blair, 1992), it was the preferred statistical procedure. There were 3 outliers in the dataset as assessed by cases of standardized residuals greater than ±3 standard deviations. The ANCOVA was run with and without outliers and statistically significant results remained unaffected. After adjustment of age

at testing and total brain segmentation volume there was a statistically significant difference between the grand average TVW measurement and injury groups, [$F(4,241) = 10.915$, $p \leq .0009$, partial $\eta^2 = 0.153$; see Table 5]. Post-hoc analysis with a Bonferroni adjustment and effect sizes were calculated (see Table 6). The severe TBI group was statistically significantly larger than the mild ($p \leq .0009$, $d = 1.17$) and control ($p \leq .0009$, $d = .87$) groups. The moderate TBI group was statistically significantly larger than the mild group ($p = .017$, $d = 1.15$) but was not statistically significantly different from the complicated mild ($p = 1.00$, $d = .31$) and control ($p = .271$, $d = .78$). Lastly, the complicated mild group was significantly larger than the mild group ($p = .001$, $d = .87$) but was not statistically different between the severe ($p = .073$, $d = .55$) or control ($p = .123$, $d = .50$) groups. There were no statistically significant difference between mild and control groups ($p = .321$, $d = -.36$; see Figure 9).

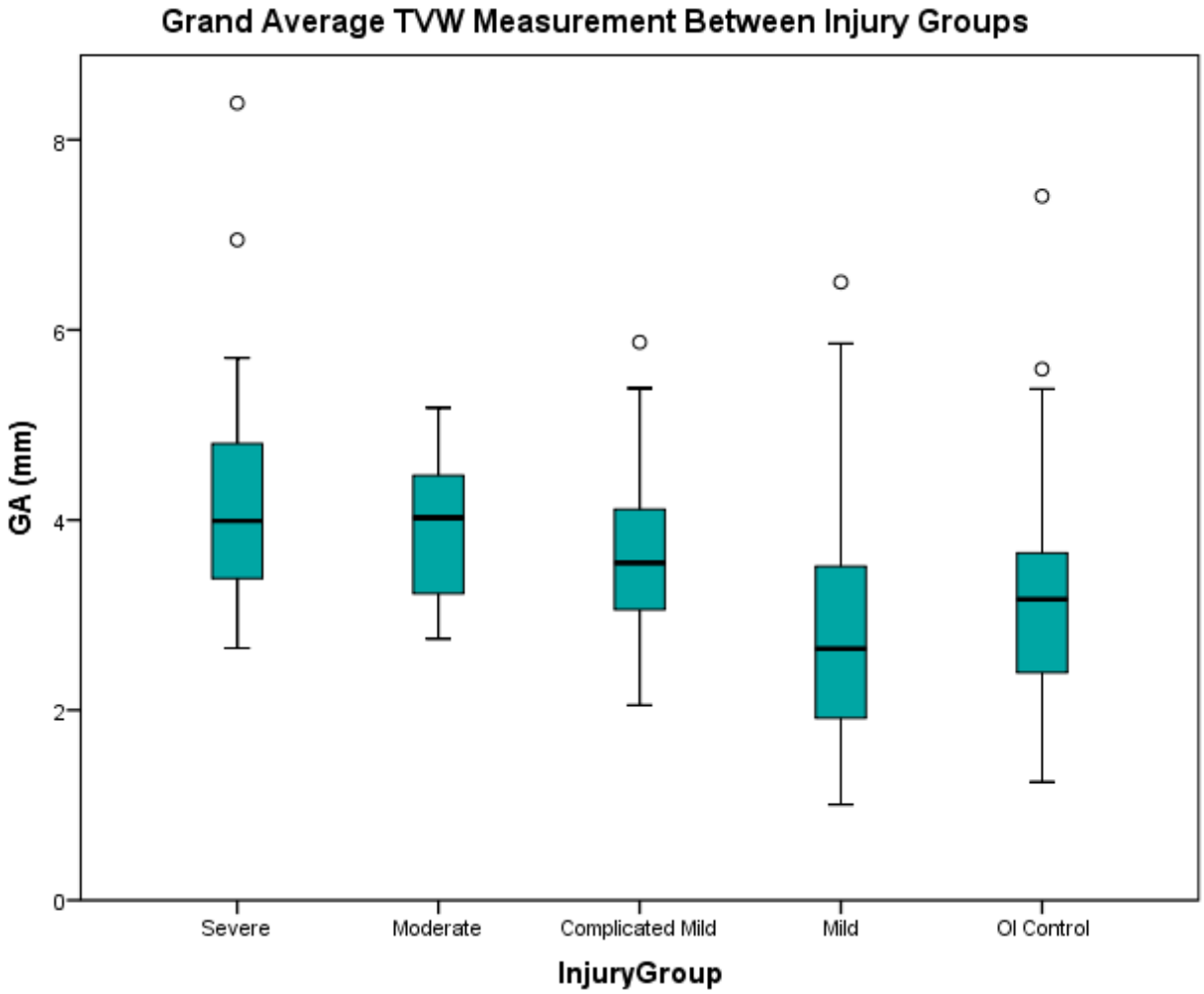

Figure 9: Grand Average TVW Means Between Subgroups. Boxplot showing between group differences for the grand average TVW measurement (GA). Center line is group median and bars represent 95% confidence intervals. The mild group was significantly smaller than the severe ($p \leq .0009$), moderate ($p = .017$), and complicated mild ($p = .001$) groups. There were no statistically significant difference between mild and control groups. Outliers represent data points approximately 1.5 standard deviations from the edge of the box according to SPSS Statistics.

Table 5: Adjusted and Unadjusted Means and Variability for Grand Average Third Ventricle Width Measurement with Total Brain Volume and Age at Testing as Covariates

		Unadjusted		Adjusted	
	N	M	SD	M	SE
Severe	19	4.327	1.489	4.486	.253
Moderate	11	3.921	.829	3.904	.322
Complicated Mild	37	3.662	.867	3.663	.175
Mild	84	2.793	1.118	2.792	.123
Control	97	3.181	1.048	3.152	.109

Note: N = number of patients, M = Mean, SD = Standard deviation, SE = Standard error. All third ventricle width metrics measured in millimeters (mm). Control group is orthopedically injured patients.

Table 6: Matrix of Cohen's d Effect Sizes Between Injury Groups

	Severe	Moderate	Complicated Mild	Mild	Control
Severe	0	.34	.55	1.17	.89
Moderate	.34	0	.31	1.15	.78
Complicated Mild	.55	.31	0	.87	.50
Mild	1.17	1.15	.87	0	-.36
Control	.89	.78	.50	-.36	0

Note: Control group is orthopedically injured patients

Hypothesis 3: The Grand Average TVW Measurement Will Predict Injury Severity Between Subgroups.

A discriminant function analysis was used. The grand average TVW as a ratio of total brain segmentation volume was the sole independent variable and injury group was the dependent variable. There was homogeneity of variances as assessed by Levene's test for homogeneity of variances ($p = .103$). There were three univariate outliers as assessed by cases of standardized residuals greater than ±3 standard deviations. The discriminant function analysis was run with and without outliers and statistically significant results were unchanged. The assumption of normality was violated as assessed individually for each group with a Shapiro-Wilk test. Moderate and complicated mild groups had $p > .05$ while the severe, mild and control groups had p-values equal to .029, .002 .003, respectively. All had a slight positive skew. Despite this the discriminant function analysis is known to be fairly robust against deviations from

normality as long as deviations are due to skewness and not outliers (Quinn & Keough, 2002; Sawilowsky & Blair, 1992), so it was the preferred statistical procedure. There was statistically significant discriminating power for the TVW measurement between specific groups (Wilk's = .779, $\chi^2 = 60.864$, $p \leq .0009$). Despite this significance, only 35.1 percent of cases were classified correctly. The grand average TVW measurement was able to best discriminate between the severe and mild subgroups, classifying 63.2 and 64.3 percent of patients correctly, respectively (See Table 7).

Table 7: Predicted Group Membership as Percentage Between Injury Groups

	Severe	Moderate	Complicated Mild	Mild	Control
Severe	63.2	0	5.3	15.8	15.8
Moderate	27.3	18.2	18.2	9.1	27.3
Complicated Mild	24.3	13.5	13.5	24.3	24.3
Mild	10.7	2.4	13.1	64.3	9.5
Control	12.4	9.3	20.6	43.3	14.4

Note: Control group is orthopedically injured patients. *35.1% percent of all cases classified correctly

Hypothesis 4: The Grand Average TVW Measurement Will Be Significantly Correlated and Comparable to Freesurfer® Derived Volumetric Outputs in Injury Group Predictability.

A Spearman's rank order correlation test was run to assess the correlation between the grand average TVW measurement and *Freesurfer*® volumetric outputs. *Freesurfer*® derived volumes included the left thalamus proper, right thalamus proper, 3rd ventricle and total brain segmentation volume. Preliminary analysis showed the relationships to be monotonic as evaluated by visual inspection of a scatterplot. There was a strong positive correlation between 3rd ventricle volume and grand average TVW, [$r_s(248) = .540$, $p \leq .0009$]. No other significant correlations were seen (see Table 10).

To assess comparability in predictive power between the grand average TVW measurement and *Freesurfer*® derived volumes a discriminant function analysis was run on each

individual measure separately (see Table 8). For detailed results see Appendix B. All values were normalized as a ratio to total brain segmentation volume. The grand average TVW was the most predictive measure correctly classifying 35.1 percent of all cases as seen in Table 8.

To determine if there was a more predictive model using a combination of measures, the grand average TVW and all *Freesurfer*® derived volumes were used as independent variables and a stepwise function was used to determine the best predictive model. There was no multicollinearity as assessed by Pearson Correlations (all r values ≤ .634). Homogeneity of variances, as assessed by Levene's test, was tested separately (See Appendix B). The grand average TVW and 3rd Ventricle volume combined made the best predictive model, predicting 39.9 percent of cases correctly, as seen in Table 9.

Table 8: Number of Cases Predicted Accurately as a Percent

	Left Thalamus Proper	Right Thalamus Proper	3rd Ventricle	BrainSegVol	GA TVW
% Correctly Classified	10.5	15.3	20.2	26.2	35.1

Note: BrainSegVol = Total brain segmentation volume, GA TVW =grand average third ventricle width

Table 9: Predicted Group Membership as Percentage Between Injury Groups With Grand Average TVW and Freesurfer® derived 3rd Ventricle Volume as Predictors

	Severe	Moderate	Complicated Mild	Mild	Control
Severe	47.4	21.1	5.3	15.8	10.5
Moderate	18.2	54.5	18.2	0	9.1
Complicated Mild	18.9	24.3	37.8	5.4	13.5
Mild	8.3	4.8	11.9	64.3	10.7
Control	11.3	12.4	18.6	41.2	16.5

Note: Control group is orthopedically injured patients. *39.9% percent of all cases classified correctly

Table 10: Spearman's Rank Order Correlation Coefficients and Significance Values with the Overall Average Third Ventricle Width Measurement

	N	Correlation Coefficients (r_s)	Significance Level (p-values)
Left Thalamus Proper	250	.011	.868
Right Thalamus Proper	250	-.049	.444
3rd Ventricle	250	.510	.000*
BrainSegVol	250	.071	.226

Note: N = number of patients, r_s = Spearman's rho, BrainSegVol = Total brain segmentation volume. *- $p \leq .0009$

DISCUSSION

Contrary to hypothesis 1; that the overall TBI group would have larger TVWs compared to the OI group was not supported and the difference non-significant (p= .267). This was likely the result of a very large number of uncomplicated mild TBI cases that were in the overall TBI sample, since there were differences when the TBI groups were examined by injury severity (see Table 5). The severe TBI subgroup statistically displayed significantly larger TVW than the OI group ($p \leq .0009$, d= .87). Out of the 151 TBI patients analyzed, only 19 received a diagnosis of severe TBI and 11 a diagnosis of moderate TBI. Another potential confounding variable could be found in the two datasets used. In the SOBIK dataset, all scans were acquired using a magnetic strength of 1.5 T However, in the UCSD study all scans were acquired using a magnetic strength of 3.0 T. Defining borders of brain structures, including the third ventricle, can be challenging due to partial volume acquisition in MRI technologies (Laidlaw, Fleischer, & Barr, 1998). Decreased resolution would potentially increase partial volume acquisition and thereby increase difficulty of defining these borders accurately. This could potential lead to scans in the SOBIK dataset being larger on average compared to the UCSD dataset due to decreased magnetic strength. The severe, moderate, and complicated mild subgroups came exclusively from the SOBIK dataset while the mild subgroup came exclusively from the UCSD dataset. The OI group was a mix of both. Lastly, it is possible there is just a lack of sensitivity in the measurement.

Consistent with the *a priori* prediction; that the grand average TVW measurement would increase at each level of injury severity, the complicated mild subgroup was significantly increased from the mild subgroup ($p \leq .0009$, $d = .87$). The literature delineates complicated mild from mild injury by the presence of a skull fracture, some form of acute intracranial hemorrhage, or identifiable edema on computed tomography (CT) in concurrence with GCS score greater than

12 (Bigler, Abildskov, et al., 2013). Since ventricular dilation is known to be an indirect measurement of atrophy (Benedict et al., 2004; Nocentini et al., 2014; Sumowski et al., 2013), and that the complicated mild group by definition has more discernable pathology on neuroimaging modalities, this result corroborates the current literature. However, since current imaging technologies are already able to distinguish between these groups with other relevant biomarkers (Bigler, Abildskov, et al., 2013), at present there is little clinical applicability in this finding.

There was also an increase in unadjusted means (see Table 5) between the complicated mild (3.66 ± .87), moderate (3.92 ± .83), and severe (4.33 ± 1.50) groups. These increases were not statistically significant however, essentially clumping all of them into one group. To assess if this was a power issue due to small sample size between specific groups, severe (n= 19) and moderate (n= 11), group effect sizes were calculated with Cohen's d. Effect sizes as assessed by Cohen's d ranged from small to moderate (see Table 6). Due to a moderate effect size between the severe and complicated mild group (d= .55), the small sample size in the severe group, could be masking potential significance between these two groups. Future investigations should look to increase the power of these groups by increasing the number of patients (Larson-Hall, 2012). Another possible explanation for the lack of demarcation between subgroups is that the measurement again is not sensitive enough. Since it was designed as a quick and efficient method to sidestep more laborious post-processing techniques, we could be losing sensitivity with an increase quickness. Future studies should consider ways to fine-tune the current protocol or novel options where time is reduced and sensitivity is maximized.

The mild group (2.79 ± 1.12) was not statistically significantly increased from the OI group (3.18 ± 1.05) with corresponding effect size as assessed by Cohen's d equal to -.36. It is

the difference between these two groups that we had particular interest in due to clinical implications. Unfortunately, contrary to the *a priori* prediction, the mild group trended towards being decreased compared to the OI group. According to the literature, traumatically-induced cerebral edema may persist for several weeks with atrophic changes potentially occurring thereafter (Blatter et al., 1997). However, this was controlled for in the experimental design, with all patients undergoing a MRI at least 6 months post-injury. In the SOBIK dataset the average time of injury to MRI scan was 2.7 years (Bigler, Yeates, et al., 2013). Another possible explanation for this decrease, and the one advocated here could be that the OI group is not representative of the control population. It is possible that the OI was not completely benign in its effects on the head and brain or prior head injuries were not mentioned on the inclusion screening, which is a specific problem in those with sports concussion (Mathias, Beall, & Bigler, 2004; Rabinowitz et al., 2015). This should be considered in future investigations where orthopedic injury patients are treated as controls.

Hypothesis 4 stated that the grand average third ventricle width measurement would be highly correlated and comparable to Freesurfer® derived volumes in injury group predictability. Since it is believed that third ventricle dilation to be indicative of thalamic atrophy at a minimum (Sumowski et al., 2013; Tiemann et al., 2009), left and right thalamus volumes were included in the analyses along with 3rd ventricle volume and total brain segmentation volume. Only the 3rd ventricle volume was statistically significantly correlated in magnitude and direction with the grand average measurement. This is a good indicator that the measurement is indeed measuring changes in third ventricle pathology.

Despite the grand average TVW only predicting 35.1% of patients correctly, it was the most predictive of injury group between all measures in the analyses (see Table 8). The

insensitivity of all measures is manifest in this analysis. A potential explanation could be to the large variances between subgroups and probable overlap (see Table 5). Future studies should again look into finding ways to increase sensitivity of the current protocol or strive for new methods that decrease time and increase sensitivity. A combination of the two most predictive factors, grand average TVW and 3rd ventricle volume, only increased predictability by 4.8%. Again still far below what is necessary for clinical implementation. It is clear that more sensitive measures are needed. Future studies might look at the 10, 50, and 90% width measurements separately. The 50% width measurement was more predictive than the most predictive model with a 41.9 percent correct classification rate (see Appendix B). This finding corroborates contemporary multiple sclerosis research that found the 50% measurement to be a robust indirect measure of atrophy in these patients (Benedict et al., 2004).

One of the principal conclusions drawn from these results is the TVW measurement's sensitivity in distinguishing the severe, moderate and complicated mild groups from the mild group as assessed by significance and effect sizes. Despite this there was also insensitivity in TVW as a prognosticator of injury group. A potential reason for this lack of sensitivity might be due to the averaging of three width measurements together. Along the length of the third ventricle, from anterior to posterior, specific anatomical areas are known to dilate first and might be more susceptible to brain atrophy (Krokfors, Katila, & Taalas, 1967). Averaging all measurements could mask the significance of one particularly sensitive area (Lo, Mamaysky, & Wang, 2000). This was shown to be true in part when the 10%, 50% and 90% width measurements were used separately in the analyses (see Appendix B). All three measures were able to delineate the mild from the OI group.

It is also interesting to note that the linear TVW measurement was more sensitive than the 3rd ventricle volume measurement. This is most likely due to lesion location. The anterior 1/3 of the third ventricle is bordered by the hypothalamus and the posterior 2/3s are bordered by the thalamus (Mortazavi et al., 2014). If, hypothetically, the damage is exclusively in the hypothalamus, a 15% increase in ventricle width would essentially be diluted to only a 5% increase in total third ventricle volume (Cousins et al., 2010). This dilution could explain the insensitivity of the 3rd ventricle volume as a measure of atrophy between groups (see Appendix B).

A general limitation of the current study is the small sample sizes of the severe (n= 19) and moderate (n= 11) injury groups. However, mTBI comprises the majority of TBIs (approximately 75-85 percent) so the composition of the different groups in this investigation does parallel real-world prevalence rates of TBI (Maas et al., 2008). Furthermore, there may not be sufficient power in the analyses to delineate the specific differences between these groups. Again it is recommended that future investigations increase the power of these groups by increasing the number of patients (Larson-Hall, 2012). Another limitation is the differences in imaging protocols. In the SOBIK dataset, all scans were acquired using a magnetic strength of 1.5 T. However, in the UCSD study all scans were acquired using a magnetic strength of 3.0 T. Defining borders of brain structures can be challenging due to partial volume acquisition in MRI technologies (Laidlaw et al., 1998). For the current study partial volume acquisition voxels were included in all width measurements. The potential consequence of this design is an increase in probability of including parenchyma in the width measurement instead of solely CSF. This could partially account for the significant increases in the complicated mild group from the mild group because all subjects came exclusively from one data set or the other.

Future investigations might consider combining this study with a VBM analysis to see if area of lesion effects a specific measurement more than others. It is already known that specific areas of the third ventricle dilate first upon incident of brain atrophy (Krokfors et al., 1967). What is unclear is why? To investigate this, future studies could us an anterior to posterior gradient to define lesion location and size. Those with anterior TBI-related lesions could be contrasted with those with more posterior lesions as to whether such pathology differentially affects third ventricle width and/or volume. For example, a lateral frontal lobe lesion might cause greater dilation in the 10% measurement compared to the 90% measurement. Or thalamic injury might cause greater dilation in the 90% compared to the 10% measurement.

In conclusion, consistent with hypothesis 2 the complicated mild injury subgroup was significantly increased from the mild injury subgroup ($p \leq .0009$, $d = .87$) which corroborates current literature (Bigler, Abildskov, et al., 2013; Williams, Levin, & Eisenberg, 1990). Contrary to hypothesis 2, the grand average TVW measurement was not sensitive enough to delineate between the severe, moderate, and complicated mild injury subgroups. Nor was it sensitive enough to delineate the mild and OI injury subgroups. Of the Freesurfer® derived volumes, the grand average TVW measurement was highly correlated with just the 3rd ventricle volume, [$r_s(248)= .540$, $p \leq .0009$]. However, despite its limitations, the grand average TVW measurement was the best prognosticator in the analyses. Future studies are needed to determine if lesion location and size effect a specific measurement compared to others.

REFERENCES

Ambarki, K., Israelsson, H., Wahlin, A., Birgander, R., Eklund, A., & Malm, J. (2010). Brain ventricular size in healthy elderly: Comparison between evans index and volume measurement. *Neurosurgery, 67*(1), 94-99. doi: 10.1227/01.neu.0000370939.30003.d1

Bauer, R., & Fritz, H. (2004). Pathophysiology of traumatic injury in the developing brain: An introduction and short update. *Experimental and Toxicologic Pathology, 56*(1-2), 65-73. doi: 10.1016/j.etp.2004.04.002

Benedict, R. H. B., Bruce, J. M., Dwyer, M. G., Abdelrahman, N., Hussein, S., Weinstock-Guttman, B., . . . Zivadinov, R. (2006). Neocortical atrophy, third ventricular width, and cognitive dysfunction in multiple sclerosis. *Archives of Neurology, 63*(9), 1301-1306. doi: 10.1001/archneur.63.9.1301

Benedict, R. H. B., Weinstock-Guttman, B., Fishman, I., Sharma, J., Tjoa, C. W., & Bakshi, R. (2004). Prediction of neuropsychological impairment in multiple sclerosis: Comparison of conventional magnetic resonance imaging measures of atrophy and lesion burden. *Archives of Neurology, 61*(2), 226-230. doi: 10.1001/archneur.61.2.226

Bigler, E. D. (2008). Neuropsychology and clinical neuroscience of persistent post-concussive syndrome. *Journal of the International Neuropsychological Society, 14*(1), 1-22. doi: 10.1017/s135561770808017x

Bigler, E. D., Abildskov, T. J., Petrie, J., Farrer, T. J., Dennis, M., Simic, N., . . . Yeates, K. O. (2013). Heterogeneity of brain lesions in pediatric traumatic brain injury. *Neuropsychology, 27*(4), 438-451. doi: 10.1037/a0032837

Bigler, E. D., Abildskov, T. J., Wilde, E. A., McCauley, S. R., Li, X. Q., Merkley, T. L., . . . Levin, H. S. (2010). Diffuse damage in pediatric traumatic brain injury: A comparison of automated versus operator-controlled quantification methods. *Neuroimage, 50*(3), 1017-1026. doi: 10.1016/j.neuroimage.2010.01.003

Bigler, E. D., & Maxwell, W. L. (2012). Neuropathology of mild traumatic brain injury: Relationship to neuroimaging findings. *Brain Imaging and Behavior, 6*(2), 108-136. doi: 10.1007/s11682-011-9145-0

Bigler, E. D., Yeates, K. O., Dennis, M., Gerhardt, C. A., Rubin, K. H., Stancin, T., . . . Vannatta, K. (2013). Neuroimaging and social behavior in children after traumatic brain injury: Findings from the Social Outcomes of Brain Injury in Kids (SOBIK) study. *Neurorehabilitation, 32*(4), 707-720. doi: 10.3233/nre-130896

Blatter, D. D., Bigler, E. D., Gale, S. D., Johnson, S. C., Anderson, C. V., Burnett, B. M., . . . Bailey, B. J. (1997). MR-based brain and cerebrospinal fluid measurement after traumatic brain injury: Correlation with neuropsychological outcome. *American Journal of Neuroradiology, 18*(1), 1-10.

Blumbergs, P. C., Scott, G., Manavis, J., Wainwright, H., Simpson, D. A., & McLean, A. J. (1994). Staining of amyloid precursor protein to study axonal damage in mild head-injury. *Lancet, 344*(8929), 1055-1056. doi: 10.1016/s0140-6736(94)91712-4

Booth, A. J., Rodgers, J. D., Schwartz, C. E., Quaranto, B. R., Weinstock-Guttman, B., Zivadinov, R., & Benedict, R. H. (2013). Active cognitive reserve influences the regional atrophy to cognition link in multiple sclerosis. *J Int Neuropsychol Soc, 19*(10), 1128-1133. doi: 10.1017/s1355617713001082

Calmon, G., & Roberts, N. (2000). Automatic measurement of changes in brain volume on consecutive 3D MR images by segmentation propagation. *Magnetic Resonance Imaging, 18*(4), 439-453. doi: 10.1016/s0730-725x(99)00118-6

Cannon, T. D., Chung, Y., He, G., Sun, D. Q., Jacobson, A., van Erp, T. G. M., . . . North Amer Prodrome Longitudinal, S. (2015). Progressive reduction in cortical thickness as psychosis develops: A multisite longitudinal neuroimaging study of youth at elevated clinical risk. *Biological Psychiatry, 77*(2), 147-157. doi: 10.1016/j.biopsych.2014.05.023

Cousins, D. A., Moore, P. B., Watson, S., Harrison, L., Ferrier, I. N., Young, A. H., & Lloyd, A. J. (2010). Pituitary volume and third ventricle width in euthymic patients with bipolar disorder. *Psychoneuroendocrinology, 35*(7), 1074-1081. doi: 10.1016/j.psyneuen.2010.01.008

Dabbs, K., Becker, T., Jones, J., Rutecki, P., Seidenberg, M., & Hermann, B. (2012). Brain structure and aging in chronic temporal lobe epilepsy. *Epilepsia, 53*(6), 1033-1043. doi: 10.1111/j.1528-1167.2012.03447.x

Dennis, M., Simic, N., Taylor, H. G., Bigler, E. D., Rubin, K., Vannatta, K., . . . Yeates, K. O. (2012). Theory of mind in children with traumatic brain injury. *Journal of the International Neuropsychological Society, 18*(5), 908-916. doi: 10.1017/s1355617712000756

Dykes, K. L., Mednick, S. A., Machon, R. A., Praestholm, J., & Parnas, J. (1992). Adult third ventricle width and infant behavioral arousal in groups at high and low risk for schizophrenia. *Schizophrenia Research, 7*(1), 13-18.

Edlow, B. L., & Wu, O. (2012). Advanced neuroimaging in traumatic brain injury. *Seminars in Neurology, 32*(4), 374-400. doi: 10.1055/s-0032-1331810

Filbey, F. M., McQueeny, T., Kadamangudi, S., Bice, C., & Ketcherside, A. (2015). Combined effects of marijuana and nicotine on memory performance and hippocampal volume. *Behavioural Brain Research, 293*, 46-53. doi: 10.1016/j.bbr.2015.07.029

Fischl, B. (2012). FreeSurfer. *Neuroimage, 62*(2), 774-781. doi: 10.1016/j.neuroimage.2012.01.021

Friston, K. J., Frith, C. D., Liddle, P. F., & Frackowiak, R. S. J. (1991). Comparing functional (PET) images: The assessment of significant change. *Journal of Cerebral Blood Flow and Metabolism, 11*(4), 690-699.

Gath, I., Jorgensen, A., Sjaastad, O., & Berstad, J. (1975). Pneumoencephalographic findings in Parkinsonism. *Archives of Neurology, 32*(11), 769-773.

Gross, R. E., Lombardi, W. J., Hutchison, W. D., Narula, S., Saint-Cyr, J. A., Dostrovsky, J. O., . . . Lozano, A. M. (1999). Variability in lesion location after microelectrode-guided pallidotomy for Parkinson's disease: Anatomical, physiological, and technical factors that determine lesion distribution. *J Neurosurg, 90*(3), 468-477. doi: 10.3171/jns.1999.90.3.0468

Groswasser, Z., Reider-Groswasser, II, Schwab, K., Ommaya, A. K., Pridgen, A., Brown, H. R., . . . Salazar, A. M. (2002). Quantitative imaging in late TBI. Part II: Cognition and work after closed and penetrating head injury: A report of the Vietnam head injury study. *Brain Injury, 16*(8), 681-690. doi: 10.1080/02699050110119835

Jovicich, J., Czanner, S., Han, X., Salat, D., van der Kouwe, A., Quinn, B., . . . Fischl, B. (2009). MRI-derived measurements of human subcortical, ventricular and intracranial brain volumes: Reliability effects of scan sessions, acquisition sequences, data analyses, scanner upgrade, scanner vendors and field strengths. *Neuroimage, 46*(1), 177-192. doi: 10.1016/j.neuroimage.2009.02.010

Kaplan, M. J., Lazoff, M., Kelly, K., Lukin, R., & Garver, D. L. (1990). Enlargement of cerebral third ventricle in psychotic patients with delayed response to neuroleptics. *Biol Psychiatry, 27*(2), 205-214.

Kempton, M. J., Stahl, D., Williams, S. C. R., & DeLisi, L. E. (2010). Progressive lateral ventricular enlargement in schizophrenia: A meta-analysis of longitudinal MRI studies. *Schizophrenia Research, 120*(1-3), 54-62. doi: 10.1016/j.schres.2010.03.036

Krokfors, G., Katila, O., & Taalas, J. (1967). Enlarged suprapineal recess of third ventricle. *Acta Neurologica Scandinavica, 43*(5), 607-&.

Laidlaw, D. H., Fleischer, K. W., & Barr, A. H. (1998). Partial-volume Bayesian classification of material mixtures in MR volume data using voxel histograms. *Ieee Transactions on Medical Imaging, 17*(1), 74-86. doi: 10.1109/42.668696

Larson-Hall, J. (2012). Our statistical intuitions may be misleading us: Why we need robust statistics. *Language Teaching, 45*, 460-474. doi: 10.1017/s0261444811000127

Lee, J. H., Yoon, S., Renshaw, P. F., Kim, T. S., Jung, J. J., Choi, Y., . . . Lyoo, I. K. (2013). Morphometric changes in lateral ventricles of patients with recent-onset type 2 diabetes mellitus. *Plos One, 8*(4), 8. doi: 10.1371/journal.pone.0060515

Lee, Y. B., & Kwon, S. J. (2009). A more detailed classification of mild head injury in adults and treatment guidelines. *Journal of Korean Neurosurgical Society, 46*(5), 451-458. doi: 10.3340/jkns.2009.46.5.451

Lemay, M., & Hochberg, F. H. (1979). Ventricular differences between hydrostatic hydrocephalus and hydrocephalus ex-vacuo by computed-tomography. *Neuroradiology, 17*(4), 191-195.

Little, D. M., Kraus, M. F., Joseph, J., Geary, E. K., Susmaras, T., Zhou, X. J., . . . Gorelick, P. B. (2010). Thalamic integrity underlies executive dysfunction in traumatic brain injury. *Neurology, 74*(7), 558-564.

Lo, A. W., Mamaysky, H., & Wang, J. (2000). Foundations of technical analysis: Computational algorithms, statistical inference, and empirical implementation. *Journal of Finance, 55*(4), 1705-1765. doi: 10.1111/0022-1082.00265

Maas, A. I. R., Stocchetti, N., & Bullock, R. (2008). Moderate and severe traumatic brain injury in adults. *Lancet Neurology, 7*(8), 728-741. doi: 10.1016/s1474-4422(08)70164-9

Maria Alvarez, R., Garcia-Diaz, L., Marquez, J., Fajardo, M., Rivas, E., Carlos Garcia-Lozano, J., & Antinolo, G. (2011). Hemimegalencephaly: Prenatal diagnosis and outcome. *Fetal Diagnosis and Therapy, 30*(3), 234-238. doi: 10.1159/000329937

Mathias, J. L., Beall, J. A., & Bigler, E. D. (2004). Neuropsychological and information processing deficits following mild traumatic brain injury. *Journal of the International Neuropsychological Society, 10*(2), 286-297. doi: 10.1017/s1355617704102117

McAllister, T. W., Ford, J. C., Ji, S., Beckwith, J. G., Flashman, L. A., Paulsen, K., & Greenwald, R. M. (2012). Maximum principal strain and strain rate associated with concussion diagnosis correlates with changes in corpus callosum white matter indices. *Annals of Biomedical Engineering, 40*(1), 127-140. doi: 10.1007/s10439-011-0402-6

Messina, D., Cerasa, A., Condino, F., Arabia, G., Novellino, F., Nicoletti, G., . . . Quattrone, A. (2011). Patterns of brain atrophy in Parkinson's disease, progressive supranuclear palsy and multiple system atrophy. *Parkinsonism & Related Disorders, 17*(3), 172-176. doi: 10.1016/j.parkreldis.2010.12.010

Mortazavi, M. M., Adeeb, N., Griessenauer, C. J., Sheikh, H., Shahidi, S., Tubbs, R. I., & Tubbs, R. S. (2014). The ventricular system of the brain: A comprehensive review of its history, anatomy, histology, embryology, and surgical considerations. *Childs Nervous System, 30*(1), 19-35. doi: 10.1007/s00381-013-2321-3

Nocentini, U., Bozzali, M., Spano, B., Cercignani, M., Serra, L., Basile, B., . . . De Luca, J. (2014). Exploration of the relationships between regional grey matter atrophy and cognition in multiple sclerosis. *Brain Imaging and Behavior, 8*(3), 378-386. doi: 10.1007/s11682-012-9170-7

Obwegeser, A. A., Uitti, R. J., Lucas, J. A., Witte, R. J., Turk, M. F., & Wharen, R. E. (2000). Predictors of neuropsychological outcome in patients following microelectrode-guided pallidotomy for Parkinson's disease. *J Neurosurg, 93*(3), 410-420. doi: 10.3171/jns.2000.93.3.0410

Ostby, Y., Tamnes, C. K., Fjell, A. M., Westlye, L. T., Due-Tonnessen, P., & Walhovd, K. B. (2009). Heterogeneity in subcortical brain development: A structural magnetic resonance imaging study of brain maturation from 8 to 30 years. *Journal of Neuroscience, 29*(38), 11772-11782. doi: 10.1523/jneurosci.1242-09.2009

Pitel, A.-L., Chanraud, S., Sullivan, E. V., & Pfefferbaum, A. (2010). Callosal microstructural abnormalities in Alzheimer's disease and alcoholism: Same phenotype, different mechanisms. *Psychiatry Research-Neuroimaging, 184*(1), 49-56. doi: 10.1016/j.pscychresns.2010.07.006

Quinn, G. P., & Keough, M. J. (2002). Experimental design and data analysis for biologists. *Experimental design and data analysis for biologists*, i-xvii, 1-537.

Rabinowitz, A. R., Li, X. Q., McCauley, S. R., Wilde, E. A., Barnes, A., Hanten, G., . . . Levin, H. S. (2015). Prevalence and predictors of poor recovery from mild traumatic brain injury. *Journal of Neurotrauma, 32*(19), 1488-1496. doi: 10.1089/neu.2014.3555

Ramasamy, D. P., Benedict, R. H. B., Cox, J. L., Fritz, D., Abdeirahman, N., Hussein, S., . . . Zivadinov, R. (2009). Extent of cerebellum, subcortical and cortical atrophy in patients with MS: A case-control study. *Journal of the Neurological Sciences, 282*(1-2), 47-54. doi: 10.1016/j.jns.2008.12.034

Rao, S. M., Glatt, S., Hammeke, T. A., McQuillen, M. P., Khatri, B. O., Rhodes, A. M., & Pollard, S. (1985). Chronic progressive multiple-sclerosis: Relationship between cerebral ventricular size and neuropsychological impairment. *Archives of Neurology, 42*(7), 678-682.

Reider, G., II, Groswasser, Z., Ommaya, A. K., Schwab, K., Pridgen, A., Brown, H. R., . . . Salazar, A. M. (2002). Quantitive imaging in late traumatic brain injury. Part I: Late imaging parameters in closed and penetrating head injuries. *Brain Inj, 16*(6), 517-525. doi: 10.1080/02699050110119141

Robb, R. A., Hanson, D. P., Karwoski, R. A., Larson, A. G., Workman, E. L., & Stacy, M. C. (1989). ANALYZE: A comprehensive, operator-interactive software package for multidimensional medical image display and analysis. *Computerized Medical Imaging and Graphics, 13*(6), 433-454. doi: 10.1016/0895-6111(89)90285-1

Rodriguez, M. J., Potter, E., Shen, Q., Barker, W., Greig-Custo, M., Agron, J., . . . Duara, R. (2012). Cognitive and structural magnetic resonance imaging features of Lewy body dementia and Alzheimer's disease. *Alzheimers & Dementia, 8*(3), 211-218. doi: 10.1016/j.jalz.2011.04.008

Ross, D. E. (2011). Review of longitudinal studies of MRI brain volumetry in patients with traumatic brain injury. *Brain Injury, 25*(13-14), 1271-1278. doi: 10.3109/02699052.2011.624568

Ruff, R. M., Camenzuli, L., & Mueller, J. (1996). Miserable minority: Emotional risk factors that influence the outcome of a mild traumatic brain injury. *Brain Injury, 10*(8), 551-565. doi: 10.1080/026990596124124

Sanchez-Benavides, G., Gomez-Anson, B., Sainz, A., Vives, Y., Delfino, M., & Pena-Casanova, J. (2010). Manual validation of FreeSurfer's automated hippocampal segmentation in normal aging, mild cognitive impairment, and Alzheimer disease subjects. *Psychiatry Research-Neuroimaging, 181*(3), 219-225. doi: 10.1016/j.pscychresns.2009.10.011

Sawilowsky, S. S., & Blair, R. C. (1992). A more realistic look at the robustness and type-II error properties of the t-test to departures from population normality. *Psychological Bulletin, 111*(2), 352-360. doi: 10.1037/0033-2909.111.2.352

Schiller, F. (1997). The cerebral ventricles: From soul to sink. *Archives of Neurology, 54*(9), 1158-1162.

Shenton, M. E., Hamoda, H. M., Schneiderman, J. S., Bouix, S., Pasternak, O., Rathi, Y., . . . Zafonte, R. (2012). A review of magnetic resonance imaging and diffusion tensor imaging findings in mild traumatic brain injury. *Brain Imaging and Behavior, 6*(2), 137-192. doi: 10.1007/s11682-012-9156-5

Sidaros, A., Skimminge, A., Liptrot, M. G., Sidaros, K., Engberg, A. W., Herning, M., . . . Rostrup, E. (2009). Long-term global and regional brain volume changes following severe traumatic brain injury: A longitudinal study with clinical correlates. *Neuroimage, 44*(1), 1-8. doi: 10.1016/j.neuroimage.2008.08.030

Sjaastad, O., Skalpe, I. O., & Engeset, A. (1969). Width of temporal horn in differential diagnosis between pressure hydrocephalus and hydrocephalus ex vacuo. *Neurology, 19*(11), 1087-&.

Smith, S. M., Jenkinson, M., Woolrich, M. W., Beckmann, C. F., Behrens, T. E. J., Johansen-Berg, H., . . . Matthews, P. M. (2004). Advances in functional and structural MR image analysis and implementation as FSL. *Neuroimage, 23*, S208-S219. doi: 10.1016/j.neuroimage.2004.07.051

Sumowski, J. F., Wylie, G. R., Leavitt, V. M., Chiaravalloti, N. D., & DeLuca, J. (2013). Default network activity is a sensitive and specific biomarker of memory in multiple sclerosis. *Multiple Sclerosis Journal, 19*(2), 199-208. doi: 10.1177/1352458512448267

Suskauer, S. J., & Huisman, T. (2009). Neuroimaging in pediatric traumatic brain injury: Current and future predictors of functional outcome. *Developmental Disabilities Research Reviews, 15*(2), 117-123. doi: 10.1002/ddrr.62

Takeuchi, H., Taki, Y., Sekiguchi, A., Nouchi, R., Kotozaki, Y., Nakagawa, S., . . . Kawashima, R. (2015). Brain structures in the sciences and humanities. *Brain Structure & Function, 220*(6), 3295-3305. doi: 10.1007/s00429-014-0857-y

Tiemann, L., Penner, I. K., Haupts, M., Schlegel, U., & Calabrese, P. (2009). Cognitive decline in multiple sclerosis: Impact of topographic lesion distribution on differential cognitive deficit patterns. *Multiple Sclerosis, 15*(10), 1164-1174. doi: 10.1177/1352458509106853

Unger, M. M., Belke, M., Menzler, K., Heverhagen, J. T., Keil, B., Stiasny-Kolster, K., . . . Knake, S. (2010). Diffusion tensor imaging in idiopathic REM sleep behavior disorder reveals microstructural changes in the brainstem, substantia nigra, olfactory region, and other brain regions. *Sleep, 33*(6), 767-773.

Wakana, S., Jiang, H. Y., Nagae-Poetscher, L. M., van Zijl, P. C. M., & Mori, S. (2004). Fiber tract-based atlas of human white matter anatomy. *Radiology, 230*(1), 77-87. doi: 10.1148/radiol.2301021640

Williams, D. H., Levin, H. S., & Eisenberg, H. M. (1990). Mild head-injury classification. *Neurosurgery, 27*(3), 422-428.

Yang, Y., Nuechterlein, K. H., Phillips, O. R., Gutman, B., Kurth, F., Dinov, I., . . . Narr, K. L. (2012). Disease and genetic contributions toward local tissue volume disturbances in schizophrenia: A tensor-based morphometry study. *Human Brain Mapping, 33*(9), 2081-2091. doi: 10.1002/hbm.21349

Zhan, W., Zhang, Y., Mueller, S. G., Lorenzen, P., Hadjidemetriou, S., Schuff, N., & Weiner, M. W. (2009). Characterization of white matter degeneration in elderly subjects by magnetic resonance diffusion and FLAIR imaging correlation. *Neuroimage, 47*, T58-T65. doi: 10.1016/j.neuroimage.2009.02.004

APPENDIX A: VISUAL PROTOCOL GUIDE

Step by Step Visual Instructions

1. Open up Osirix program on designated Mac computer and import desired DICOM images into Osirix program. Hit the import button in the top left corner as indicated by the blue arrows.

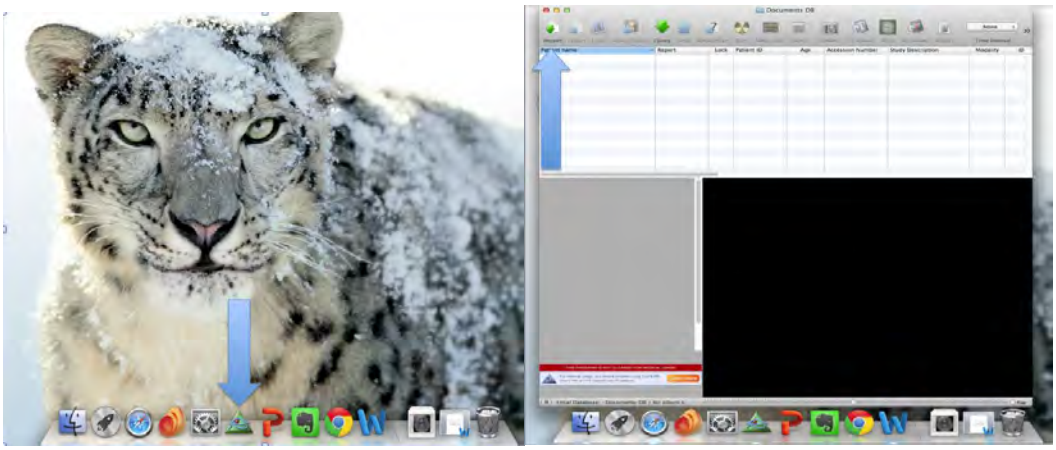

2. Once the images have been loaded you should have a screen similar to the image shown below.

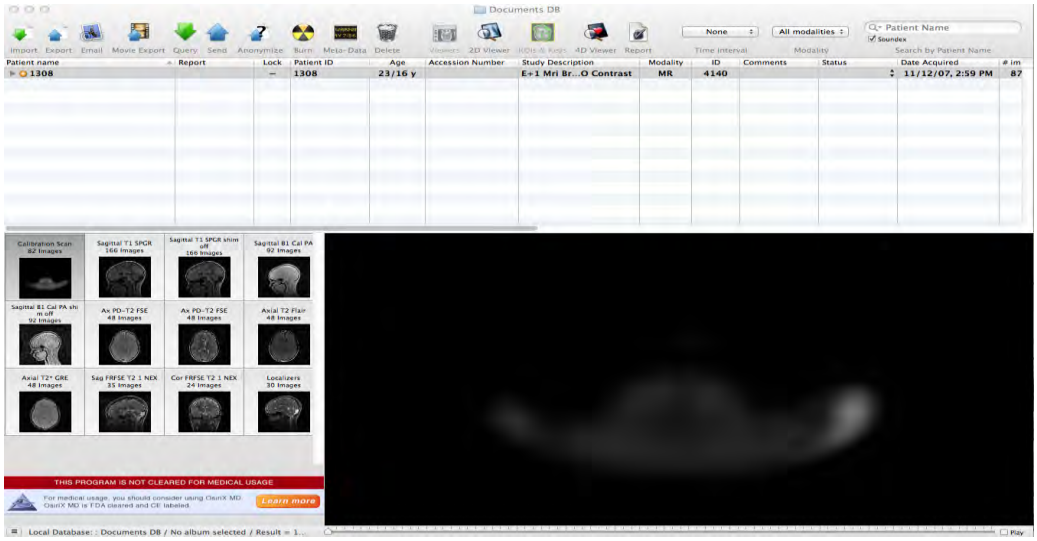

3. Double click on the desired MRI sequence. In this study the Axial T2 image was used in the SOBIK data set and the FLAIR in the UCSD data set.

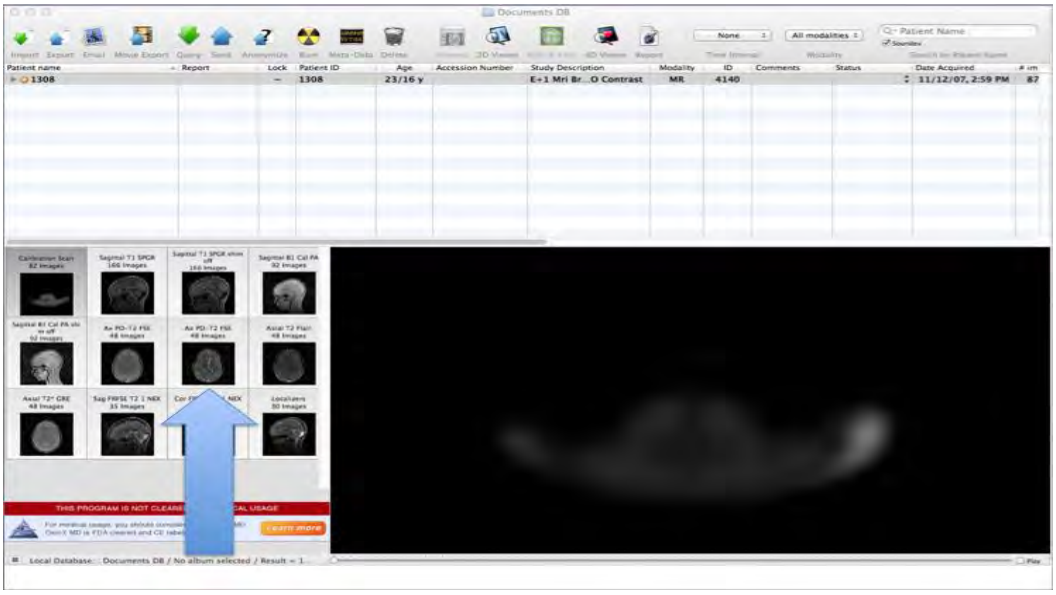

4. A screen should open with the specific sequence visible as shown below.

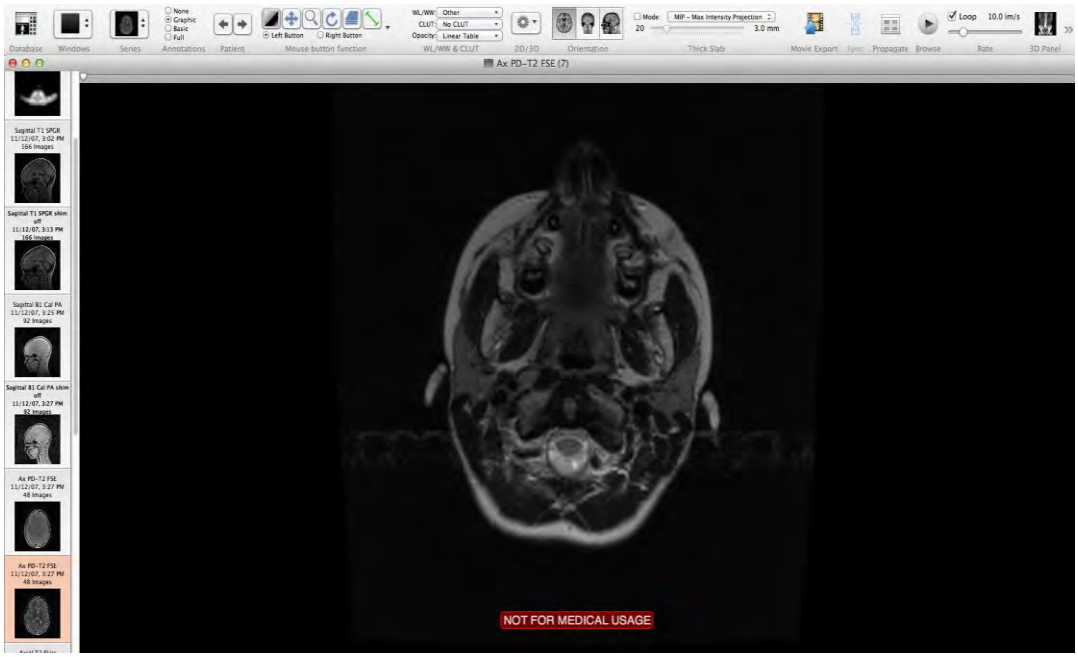

5. Using the scroll tool, scroll dorsally until the third ventricle is visible and no part of the midbrain in visible. This slice should correspond to a continuous view of the third ventricle below the interthalamic adhesion as shown below. Exceptions apply (see end of this appendix).

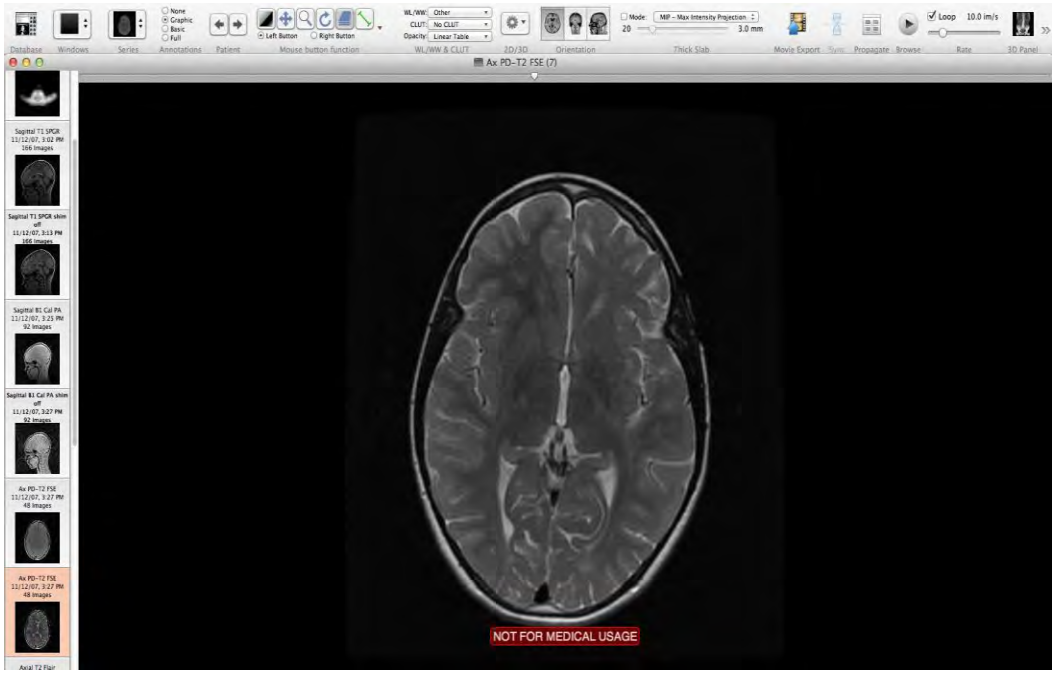

6. Using the magnifying tool, zoom in on third ventricle until we have a clear view of its boundaries. Using the line tool, draw a line region of interest (ROI) through the long axis of the third ventricle, parallel with the interhemispheric fissure. Start on the anterior dark boundary (white boundary if on the FLAIR) of the third ventricle and end on the posterior dark boundary of the third ventricle. Be sure to include partial volume acquisition voxels. The resulting image should look as follows.

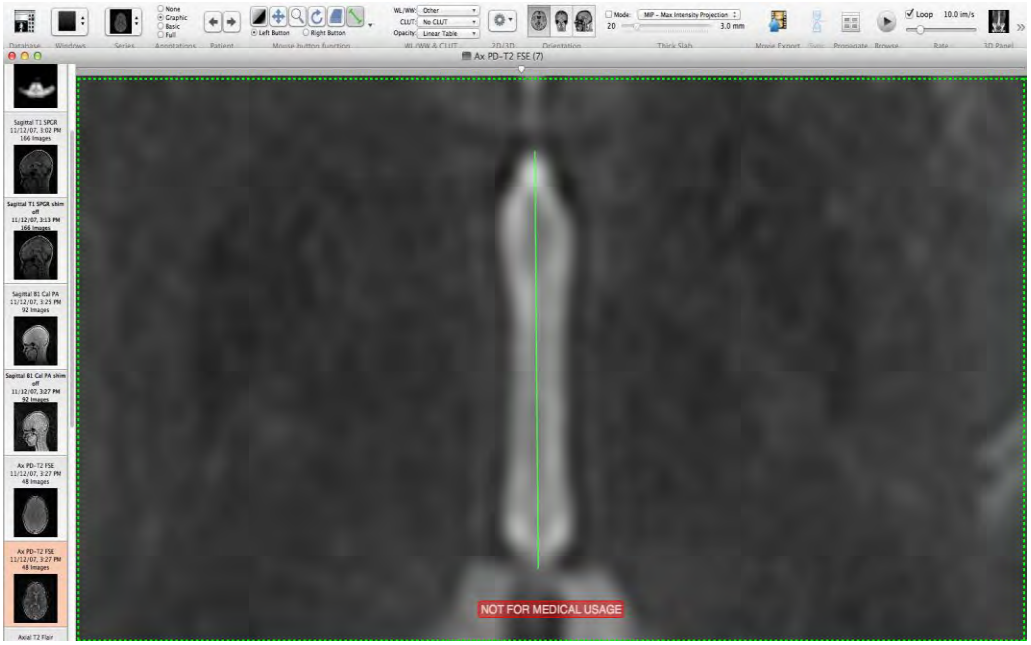

7. In order to quickly calculate the 10, 50 and 90% measurements, click in the middle of the ROI just drawn and drag slightly to the right. This line will now serve as a template for the next line.

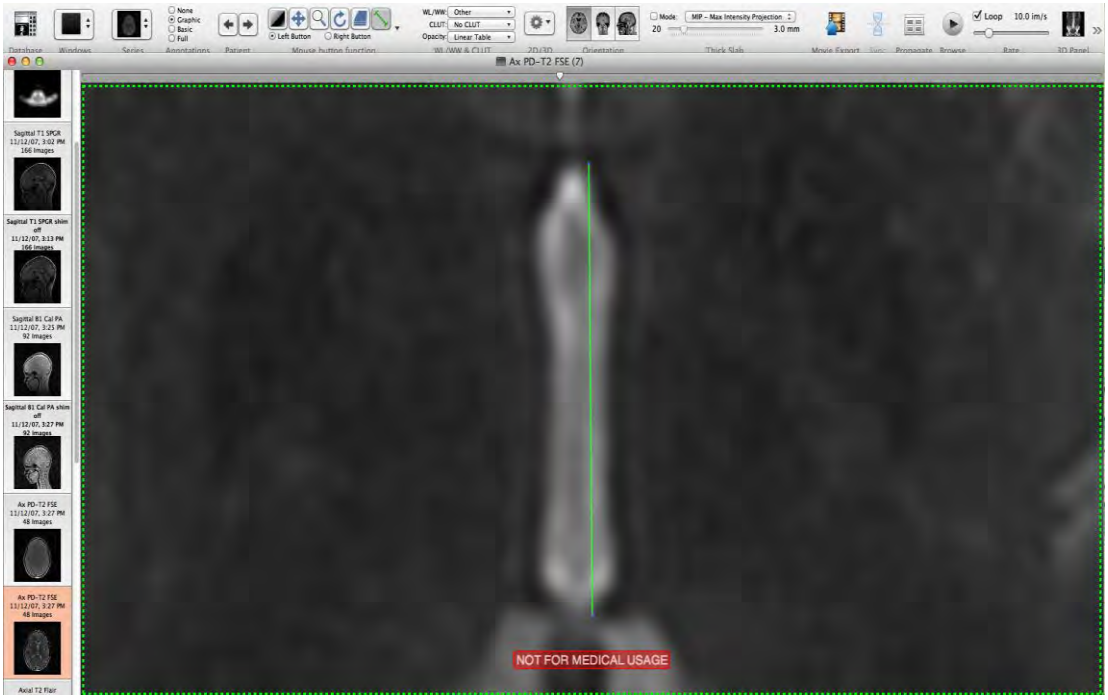

8. Now draw the same line starting in the same spot as the first but only going 10% of the first line. Draw another little line off to the left as the 10% horizontal maker as shown below.

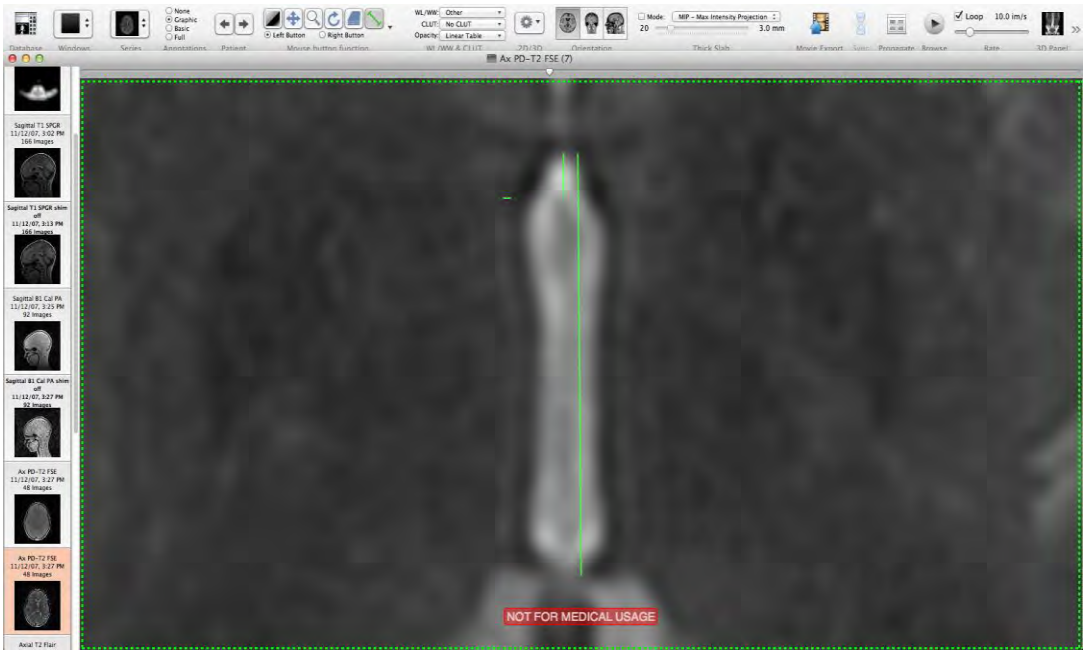

9. Do this again for the 50 and 90% percent horizontal markers. Once the makers are in place we can delete the second vertical line. The resulting image should appear has follows.

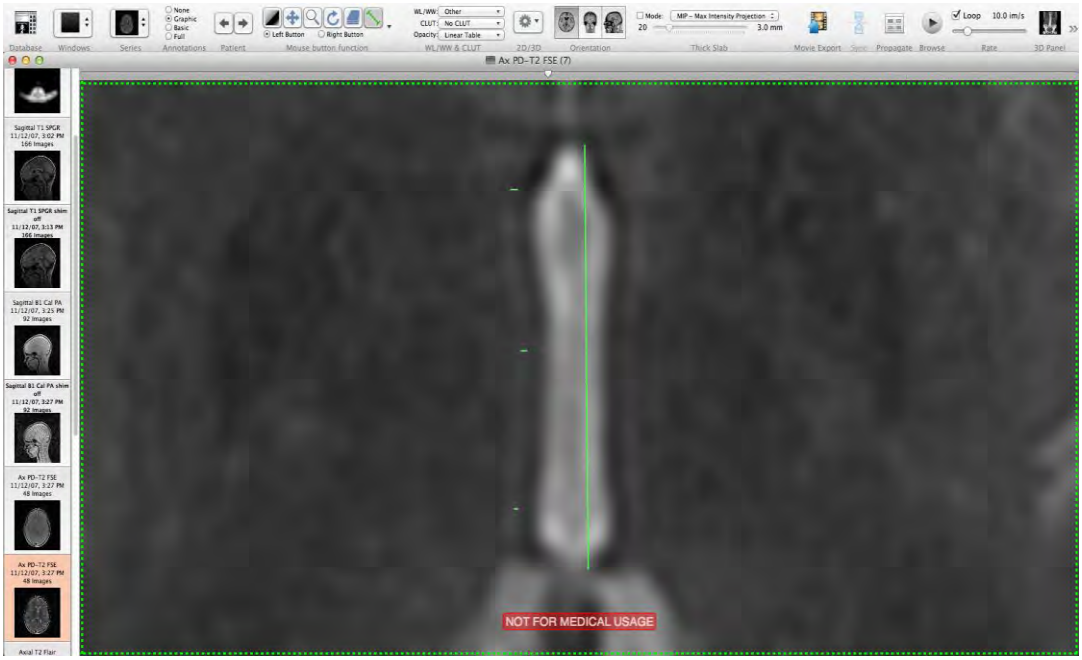

10. Move the original vertical line to the right so that it is out of the third ventricle CSF and draw the three width measurements next to the horizontal markers. As with the ventricle length ROI, go from dark boundary to dark boundary (light boundary to light boundary if FLAIR) making sure to include partial volume acquisition voxels. Lining up the width measurements with the horizontal markers is not exact but we can approximate fairly accurately.

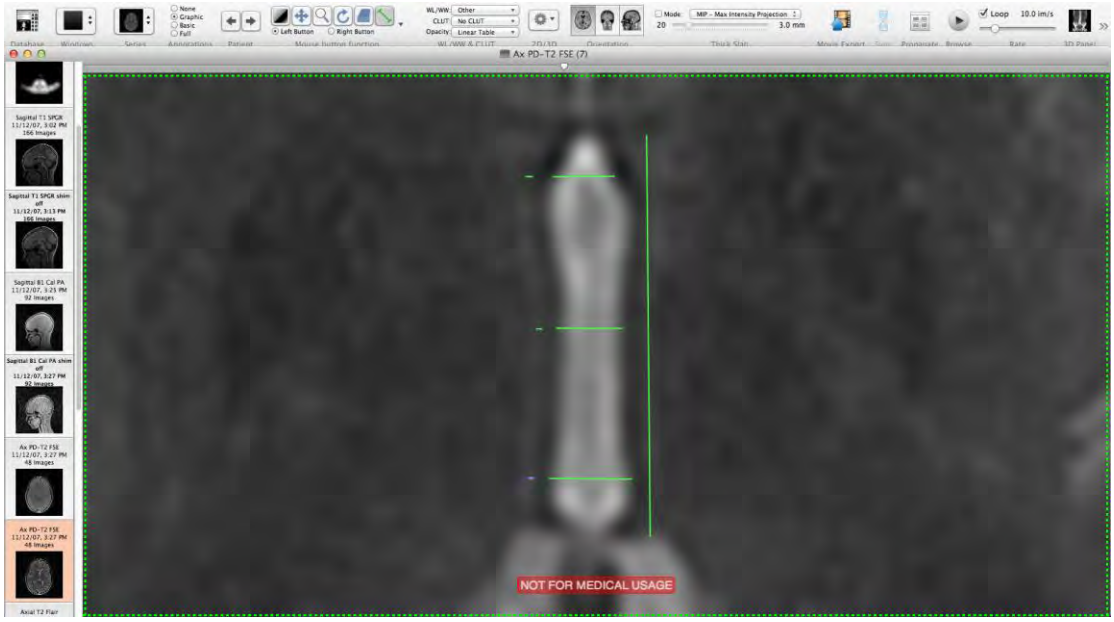

11. Record measurements in excel spreadsheet and you are done!

Exceptions

Starting with step 5, when scrolling to find the proper slice, if part of the midbrain is visible and the anterior commissure and posterior commissure are both visible this will be the trump slice. Shown below are examples where the tectum of the midbrain is visible along with both the anterior commissure (AC) and posterior commissure (PC). Instead of scrolling dorsally one slice until no part of the midbrain is visible, measurements are taken on this slice.

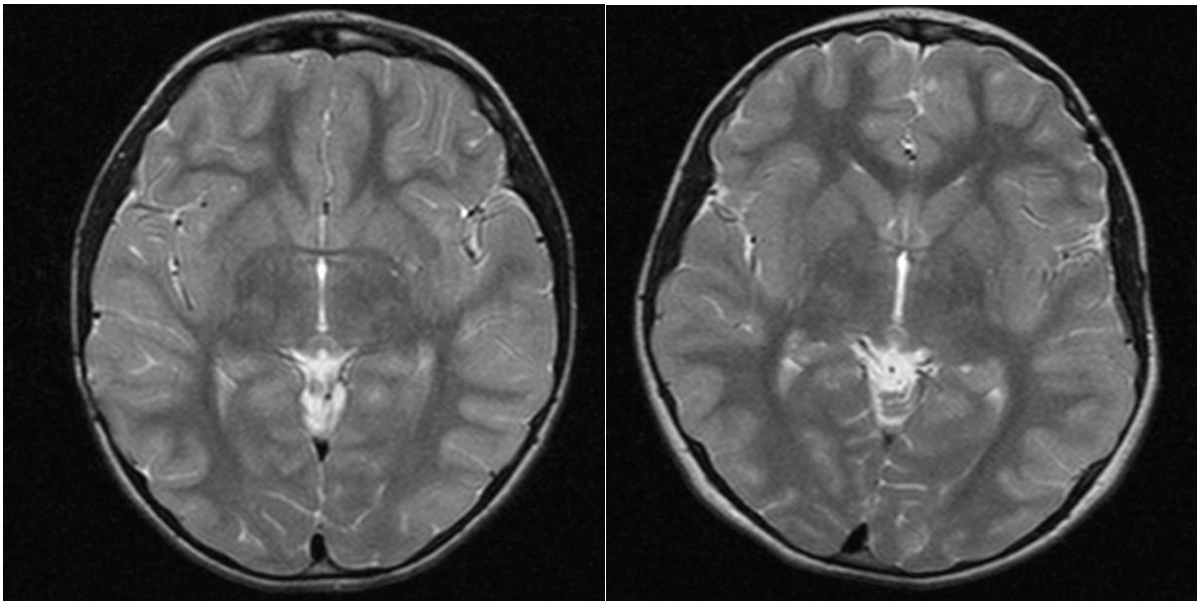

Below are some examples of where just one of the commissures is visible. In the one on the left the PC is not visible and on the right the AC is not visible. On both of these cases, we would scroll dorsally one more slice until no part of the midbrain is visible.

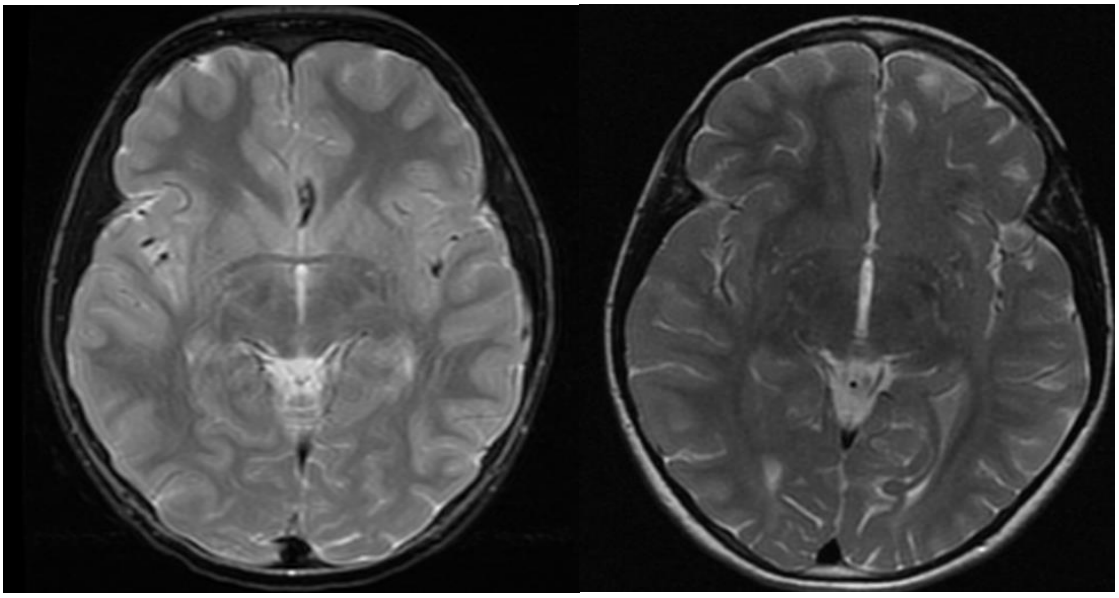

Also in rare cases, the optimal slice is one slice superior to the slice where no midbrain is visible. For good measure check one slice superior and inferior to the default slice.

APPENDIX B: ADDITIONAL STATISTICS

10% TVW Measure

The assumption of homogeneity of variances was violated so a one-way Welch's ANOVA with a Games-Howell post hoc test was run instead of the ANCOVA. Total brain volume was controlled by normalizing all values as a ratio to total brain volume (Filbey et al., 2015). There was a linear relationship between the 10% TVW measurement, and covariates, age at testing and brain segmentation volume, as assessed by visual inspection of a scatterplot. Homogeneity of regression slopes was confirmed as both interaction terms, ageattesting*injurygroup and brainsegvol*injurygroup, were not statistically significant, [F (4,233) = .926, p= .450, F (4,233) = .178, p= .949, respectively]. Standardized residuals for individual groups and the overall model were normally distributed, as assessed by a Shapiro-Wilk test (p> .05). There was one outlier in the dataset as assessed by cases of standardized residuals greater than ±3 standard deviations. The one-way ANOVA was run with and without this outlier and statistically significant results were unchanged. The 10% TVW measure was statistically significantly different between injury groups, [Welch's F(4,46.317) = 24.629, p≤ .0009[. The Games-Howell post hoc test revealed that the mild group was significantly smaller from the severe group (p≤ .0009), moderate group (p= .002), complicated mild group (p≤ .0009), and the OI group (p≤ .0009). Also that the OI was significantly smaller from the severe (p= .010) and complicated mild group (p=.016) but not the moderate group (p= .084). No other significant differences were observed (see Table 11 and Figure 10). Prognostic power shown in Table 12.

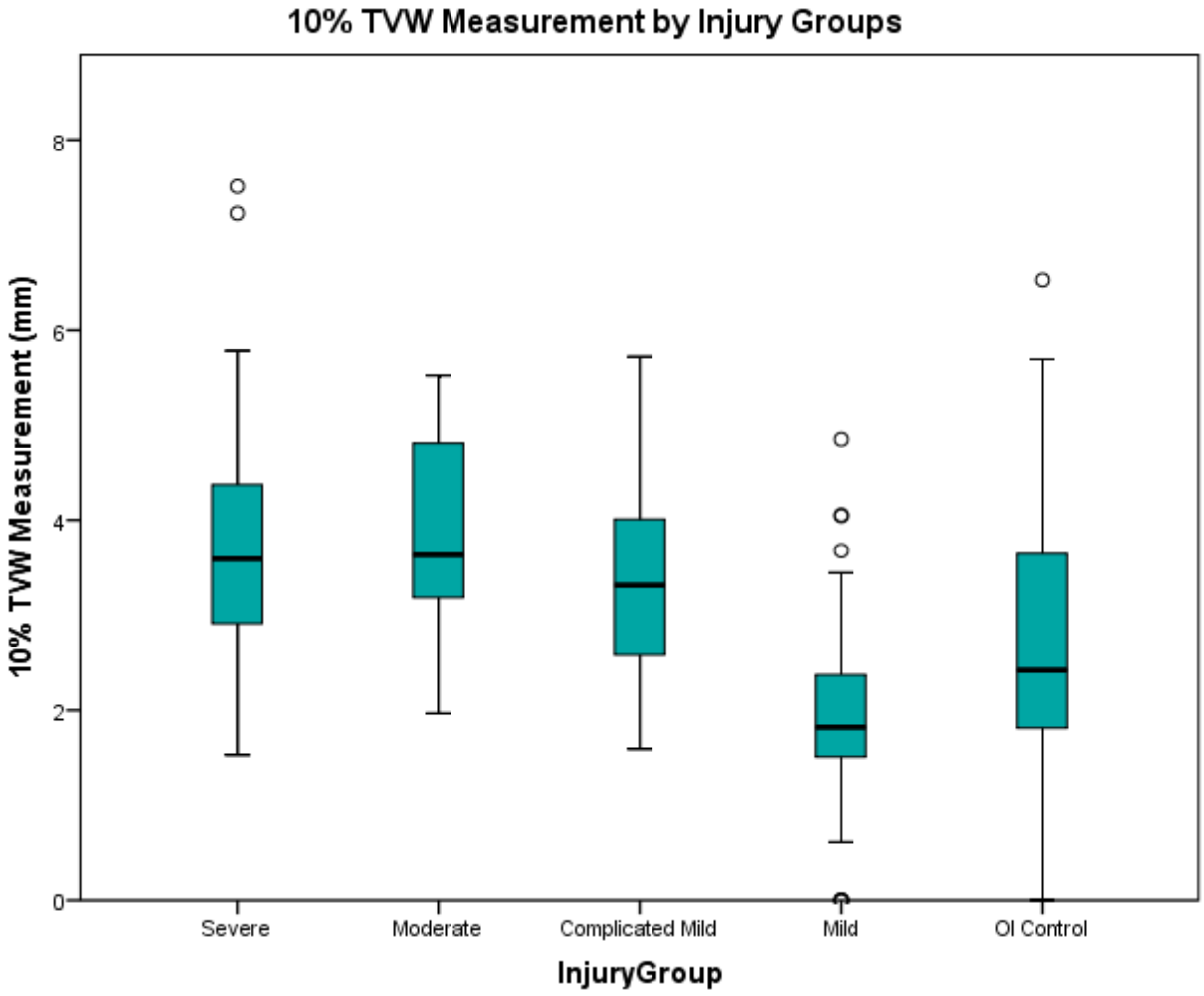

Figure 10: 10% TVW Means Between Subgroups. Boxplot showing between group differences for the 10% TVW measurement. Center line is group median and bars represent 95% confidence intervals. The mild group was statistically significantly decreased from the severe ($p \leq .0009$), moderate ($p = .002$), and complicated mild ($p \leq .0009$), and OI ($p \leq .0009$) groups. OI groups was also statistically significantly decreased from the severe ($p = .010$) and complicated mild ($p = .028$) groups. Outliers represent data points greater than or equal to 1.5 standard deviations from mean for boxplot only.

Table 11: Adjusted and Unadjusted Measurement Means and Variability for 10% TVW Measurement

		Unadjusted		Adjusted	
	N	M	SD	M	SE
Severe	19	3.895	1.639	4.022	.275
Moderate	11	3.789	1.178	3.762	.350
Complicated Mild	37	3.343	1.009	3.338	.191
Mild	84	1.927	.933	1.938	.134
Control	97	2.709	1.285	2.679	.118

Note: N = number of patients, M = Mean, SD = Standard deviation, SE = Standard error. All linear metrics are measured in millimeters (mm).

Table 12: Predicted Group Membership as Percentage Between Injury Groups

	Severe	Moderate	Complicated Mild	Mild	Control
Severe	42.1	15.8	21.1	5.3	15.8
Moderate	36.4	18.2	27.3	18.2	0
Complicated Mild	32.4	10.8	18.9	16.2	21.6
Mild	2.4	2.4	3.6	72.6	19.0
Control	15.5	11.3	13.4	44.3	15.5

Note: Control group is orthopedically injured patients. *37.5% percent of all cases classified correctly

50% TVW Measure

The assumption of homogeneity of variances was violated so a one-way Welch's ANOVA with a Games-Howell post hoc test was run instead of the ANCOVA. Total brain volume was controlled by normalizing all values as a ratio to total brain volume (Filbey et al., 2015). There was a linear relationship between the 50% TVW measurement, and covariates, age at testing and brain segmentation volume, as assessed by visual inspection of a scatterplot. Homogeneity of regression slopes was confirmed as both interaction terms, ageattesting*injurygroup and brainsegvol*injurygroup, were not statistically significant, [F (4,233) = .496, p= .739, F (4,233) = 1.376, p= .243, respectively]. Standardized residuals for individual groups and the overall model violated the assumption of normality as assessed by a Shapiro-Wilk test. The severe and moderate groups were normally distributed (p> .05) while the

complicated mild, mild, and OI groups were not, p= .024, p≤ .0009, p≤ .0009, respectively. Despite this, since one-way ANOVA is known to be fairly robust against deviations from normality, especially when groups are skewed in similar ways (Sawilowsky & Blair, 1992), it was the preferred statistical procedure. There were two outliers in the dataset as assessed by cases of standardized residuals greater than ±3 standard deviations. The one-way ANOVA was run with and without these outliers and statistically significant results were unaffected. The 50% TVW measure was statistically significantly different between injury groups, [Welch's $F(4,45.914) = 20.489$, p≤ .0009]. The Games-Howell post hoc test revealed that the mild group was statistically significantly smaller compared with the severe group (p= .001), moderate group (p= .008), complicated mild group (p≤ .0009), and the OI group (p≤ .0009). Also that the OI was statistically significantly smaller than complicated mild (p≤ .0009) groups but not the severe (p= .060) or moderate (p= .386) groups. No other significant differences were observed (see Table 13 and Figure 11). Prognostic power shown in Table 14.

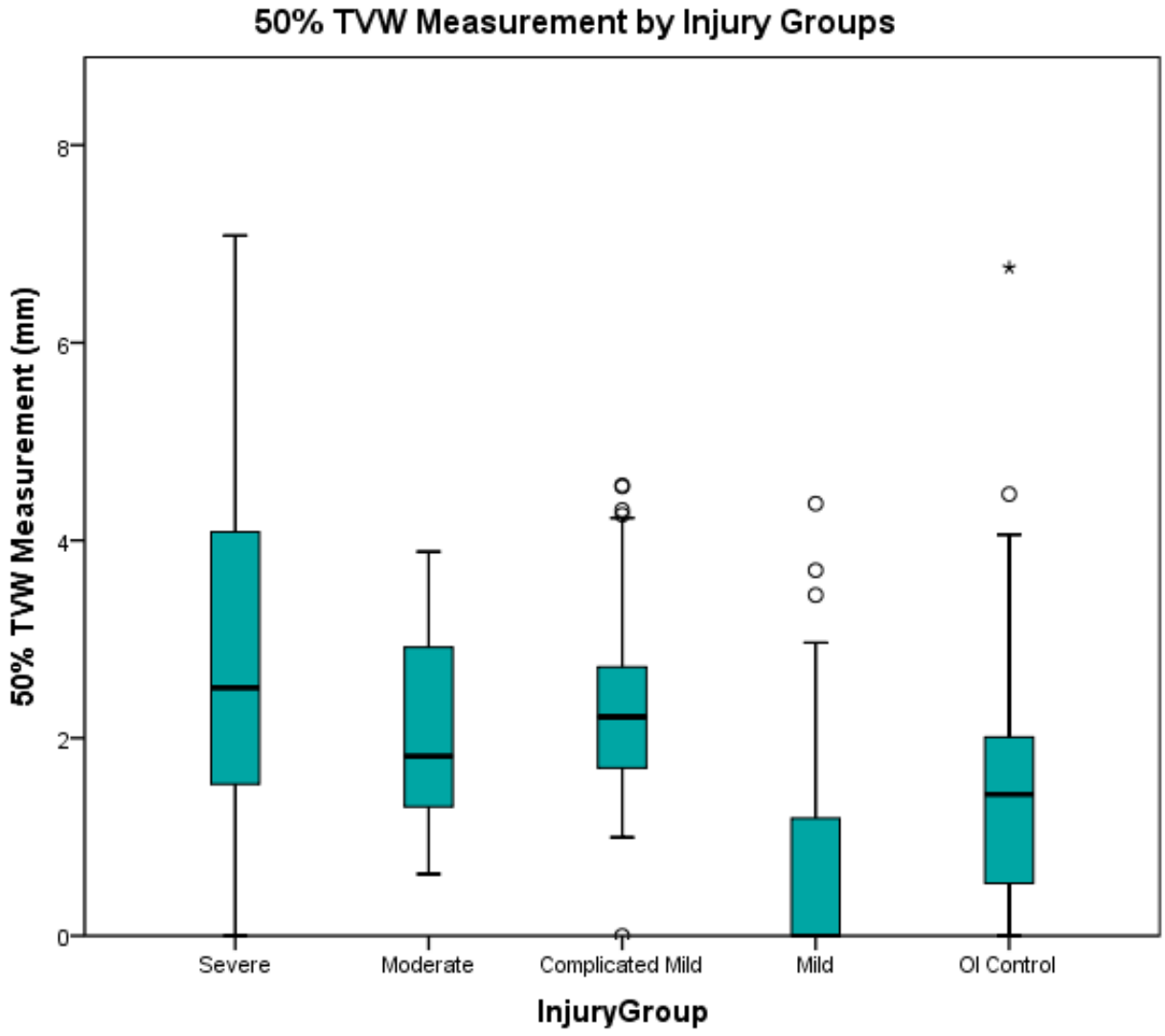

Figure 11: 50% TVW Means Between Subgroups. Boxplot showing between group differences for the 50% TVW measurement. Center line is group median and bars represent 95% confidence intervals. The mild group was statistically significantly decreased from the severe ($p = .001$), moderate ($p = .010$), and complicated mild ($p \leq .0009$), and OI ($p \leq .0009$) groups. OI groups was also statistically significantly decreased from the severe ($p = .031$) and complicated mild ($p \leq .0009$) groups. Outliers represent data points greater than or equal to 1.5 standard deviations from mean for boxplot only.

Table 13: Adjusted and Unadjusted Measurement Means and Variability for 50% TVW Measurement

		Unadjusted		Adjusted	
	N	M	SD	M	SE
Severe	19	2.731	1.831	2.880	.277
Moderate	11	2.137	1.125	2.103	.352
Complicated Mild	37	2.414	1.052	2.407	.192
Mild	84	.611	.926	.627	.135
Control	97	1.465	1.266	1.429	.119

Note: N = number of patients, M = Mean, SD = Standard deviation, SE = Standard error. All linear metrics are measured in millimeters (mm).

Table 14: Predicted Group Membership as Percentage Between Injury Groups

	Severe	Moderate	Complicated Mild	Mild	Control
Severe	47.4	5.3	10.5	15.8	21.1
Moderate	27.3	0	18.2	27.3	27.3
Complicated Mild	32.4	32.4	10.8	2.7	21.6
Mild	3.6	2.4	1.2	73.8	19.0
Control	15.5	13.4	3.1	38.1	29.9

Note: Control group is orthopedically injured patients. *41.9% percent of all cases classified correctly

90% TVW Measure

An ANCOVA was used for analysis. There was a linear relationship between the 90% TVW measurement, and covariates, age at testing and brain segmentation volume, as assessed by visual inspection of a scatterplot. Homogeneity of regression slopes was confirmed as both interaction terms, ageattesting*injurygroup and brainsegvol*injurygroup, were not statistically significant, [F (4,233) = .971, p= .424, F (4,233) = .581, p= .677, respectively]. There was homoscedasticity and homogeneity of variances as assessed by visual inspection of a scatterplot and Levene's test for homogeneity of variances (p= .139), respectively. Standardized residuals did not meet the assumption of normality between all groups however as assessed with a Shapiro-Wilk test. All groups had p> .05 while the mild group had p= .013. The normality of

standardized residuals for the overall model also did not meet this assumption, as assessed with a Shapiro-Wilk test, p= .001. Despite this, the ANCOVA is known to be fairly robust against deviations from normality, especially when groups are skewed in similar ways. Therefore it was the preferred statistical procedure. The ANCOVA was run with and without outliers and statistically significant results remained mostly unaffected. One additional result was found as described below. After adjustment of age at testing and brain segmentation volume there was a statistically significant difference between the 90% TVW measurement and injury groups, [$F(4,241) = 17.296$, $p \leq .0009$, partial $\eta^2 = 0.223$; see Table 15]. Post-hoc analysis with a Bonferroni adjustment was performed. The severe TBI group was statistically significantly larger than the mild ($p \leq .0009$) and control ($p \leq .0009$) groups. The moderate TBI group was statistically significantly increased the mild group ($p \leq .0009$) but not the control group ($p = .057$). Without the outliers the moderate group was also significantly larger than the control group ($p = .023$). The complicated mild group was statistically significantly larger to the mild ($p \leq .0009$) and control ($p = .017$) groups. It was not however statistically significantly different from the severe ($p = .075$) or moderate ($p = 1.00$) groups. Lastly, the mild group was significantly decreased to the control group ($p = .007$). For representative boxplot see Figure 12. Prognostic power shown in Table 16.

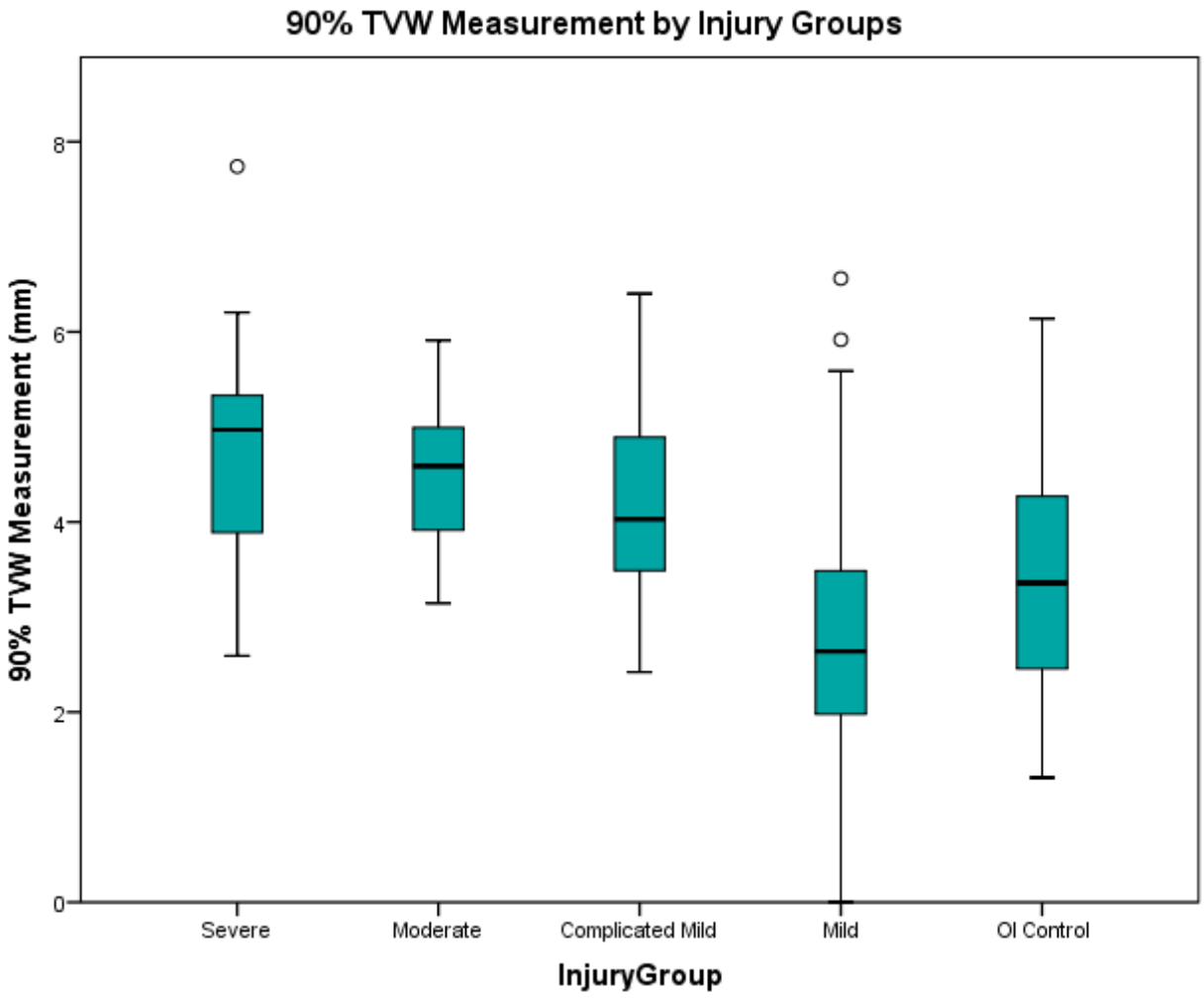

Figure 12: 90% TVW Means Between Subgroups. Boxplot showing between group differences for the 90% TVW measurement. Center line is group median and bars represent 95% confidence intervals. The mild group was significantly decreased compared to the severe ($p \leq .0009$), moderate ($p \leq .0009$), and complicated mild ($p \leq .0009$), and OI ($p = .007$) groups. OI groups was also statistically significantly decreased from the severe ($p \leq .0009$) and complicated mild ($p = .017$) groups with outliers present. With outliers in analysis the control group is significantly decreased to the moderate group ($p = .023$) as well. Outliers represent data points greater than or equal to 1.5 standard deviations from mean for boxplot only.

Table 15: Adjusted and Unadjusted Measurement Means and Variability for 90% TVW Measurement with Brain Segmentation Volume and Age at Testing as Covariates

		Unadjusted		Adjusted	
	N	M	SD	M	SE
Severe	19	4.947	1.606	5.058	.279
Moderate	11	4.510	.860	4.476	.355
Complicated Mild	37	4.163	.965	4.154	.193
Mild	84	2.781	1.143	2.800	.136
Control	97	3.467	1.216	3.436	.120

Note: N = number of patients, M = Mean, SD = Standard deviation, SE = Standard error. All linear metrics are measured in millimeters (mm).

Table 16: Predicted Group Membership as Percentage Between Injury Groups

	Severe	Moderate	Complicated Mild	Mild	Control
Severe	63.2	0	15.8	10.5	10.5
Moderate	18.2	36.4	18.2	0	27.3
Complicated Mild	24.3	16.2	16.2	8.1	35.1
Mild	3.6	6.0	4.8	70.2	15.5
Control	11.3	13.4	13.4	44.3	17.5

Note: Control group is orthopedically injured patients. *39.5% percent of all cases classified correctly

3rd Ventricle Volume

The assumption of homogeneity of variances was violated so a one-way Welch's ANOVA with a Games-Howell post hoc test was run instead of the ANCOVA. Total brain volume was controlled by normalizing all values as a ratio to total brain volume. There was a linear relationship between Freesurfer® derived 3rd ventricle volume, and covariates, age at testing and brain segmentation volume, as assessed by visual inspection of a scatterplot. Homogeneity of regression slopes was confirmed as both interaction terms, ageattesting*injurygroup and brainsegvol*injurygroup, were not statistically significant, [F (4,233) = .261, p= .903, F (4,233) = .616, p= .651, respectively]. Standardized residuals did not meet the assumption of normality between all groups as assessed with a Shapiro-Wilk test. The moderate and complicated mild groups had a p> .05 while the severe, mild, and OI groups had

p= .041, p≤ .0009, p≤ .0009, respectively. The normality of standardized residuals for the overall model also did not meet this assumption, as assessed with a Shapiro-Wilk test, p≤ .0009. Despite this, the one-way ANOVA is known to be fairly robust against deviations from normality, especially when groups are skewed in similar ways. The one-way ANOVA was run with and without this outlier and statistically significant results were driven by these outliers. There was no statistically significant differences between groups when outliers are removed, [Welch's F(4,44.772) = 1.688, p= .170; see Figure 13 and Table 17]. Prognostic power shown in Table 18.

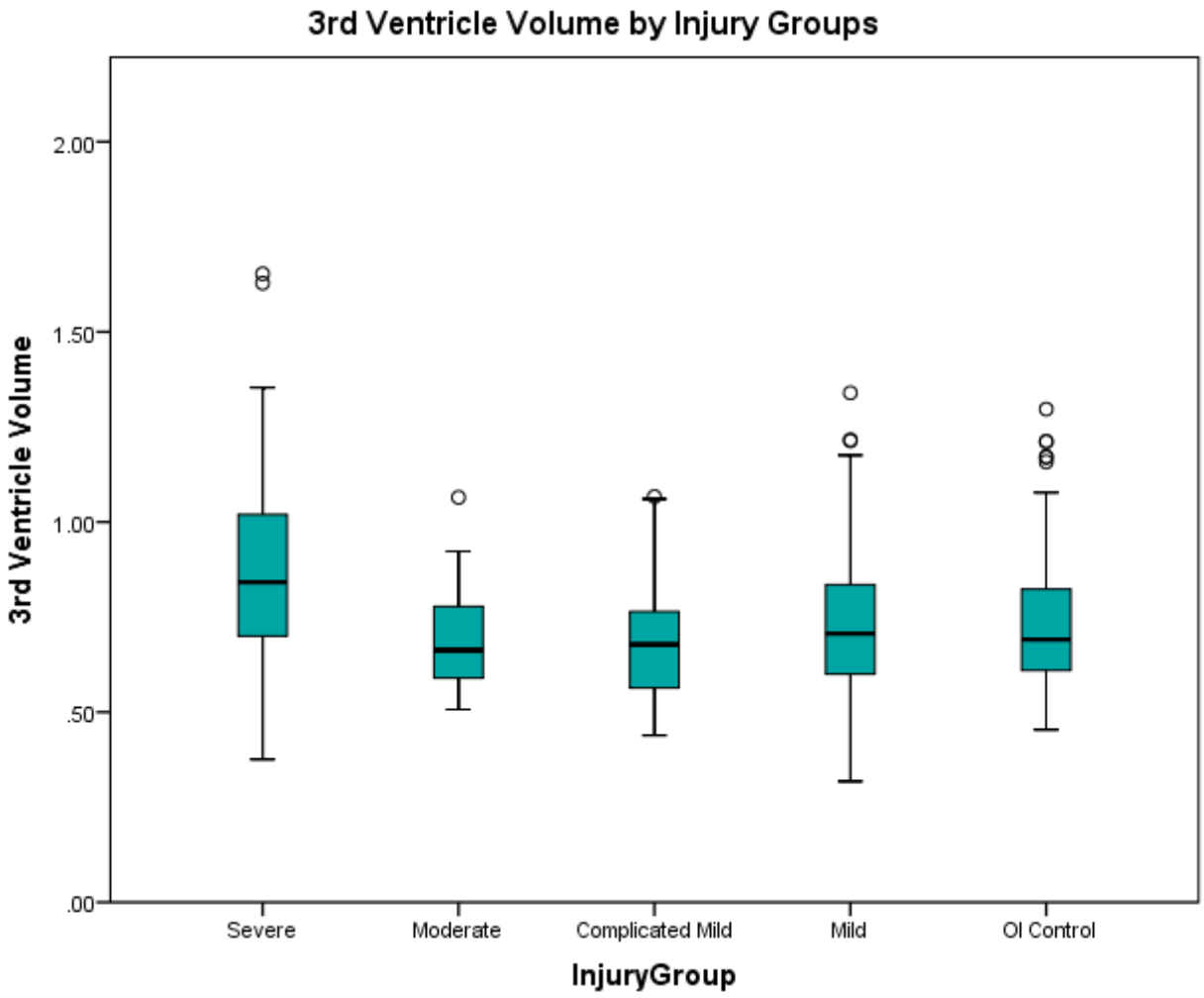

Figure 13: 3rd Ventricle Volume Means Between Subgroups. Boxplot showing between group differences for the 3rd ventricle volume measurement. Volume measured in cm^3. Center line is group median and bars represent 95% confidence intervals. There were no significant differences between groups. Outliers represent data points greater than or equal to 1.5 standard deviations from mean for boxplot only.

Table 17: Adjusted and Unadjusted Measurement Means and Variability for 3rd Ventricle Volume

		Unadjusted		Adjusted	
	N	M	SD	M	SE
Severe	19	.908	.333	.964	.053
Moderate	11	.710	.172	.719	.067
Complicated Mild	37	.703	.179	.710	.037
Mild	84	.752	.211	.739	.026
Control	97	.769	.239	.765	.023

Note: N = number of patients, M = Mean, SD = Standard deviation, SE = Standard error. All linear metrics are measured in millimeters (cm^3).

Table 18: Predicted Group Membership as Percentage Between Injury Groups

	Severe	Moderate	Complicated Mild	Mild	Control
Severe	52.6	0	31.6	0	15.8
Moderate	18.2	0	63.6	0	18.2
Complicated Mild	21.6	0	54.1	0	24.3
Mild	19.0	4.8	50.0	7.1	19.0
Control	22.7	7.2	49.5	6.2	14.4

Note: Control group is orthopedically injured patients. *20.2% percent of all cases classified correctly

Left Thalamus Measure

An ANCOVA was used for analysis. There was a linear relationship between left thalamus volume, and covariates, age at testing and brain segmentation volume, as assessed by visual inspection of a scatterplot. Homogeneity of regression slopes was confirmed as both interaction terms, ageattesting*injurygroup and brainsegvol*injurygroup, were not statistically significant, [F (4,233) = .324, p= .862, F (4,233) = 1.945, p= .104, respectively]. There was homogeneity of variances as assessed by Levene's test for homogeneity of variances (p= .225). Standardized residuals for individual groups and the overall model were normally distributed, as assessed by a Shapiro-Wilk test (p> .05). There were one outlier in the dataset as assessed by cases of standardized residuals greater than ±3 standard deviations. The ANCOVA was run with and without the outliers and statistically significant results remained unaffected. After adjustment of age at testing and brain segmentation volume there was no statistically significant difference between the left thalamus volume measurement and injury groups, [F(4,241) = .310, p=.871, partial $\eta^2 = 0.005$; see Figure 14 and Table 19]. Prognostic power shown in Table 20.

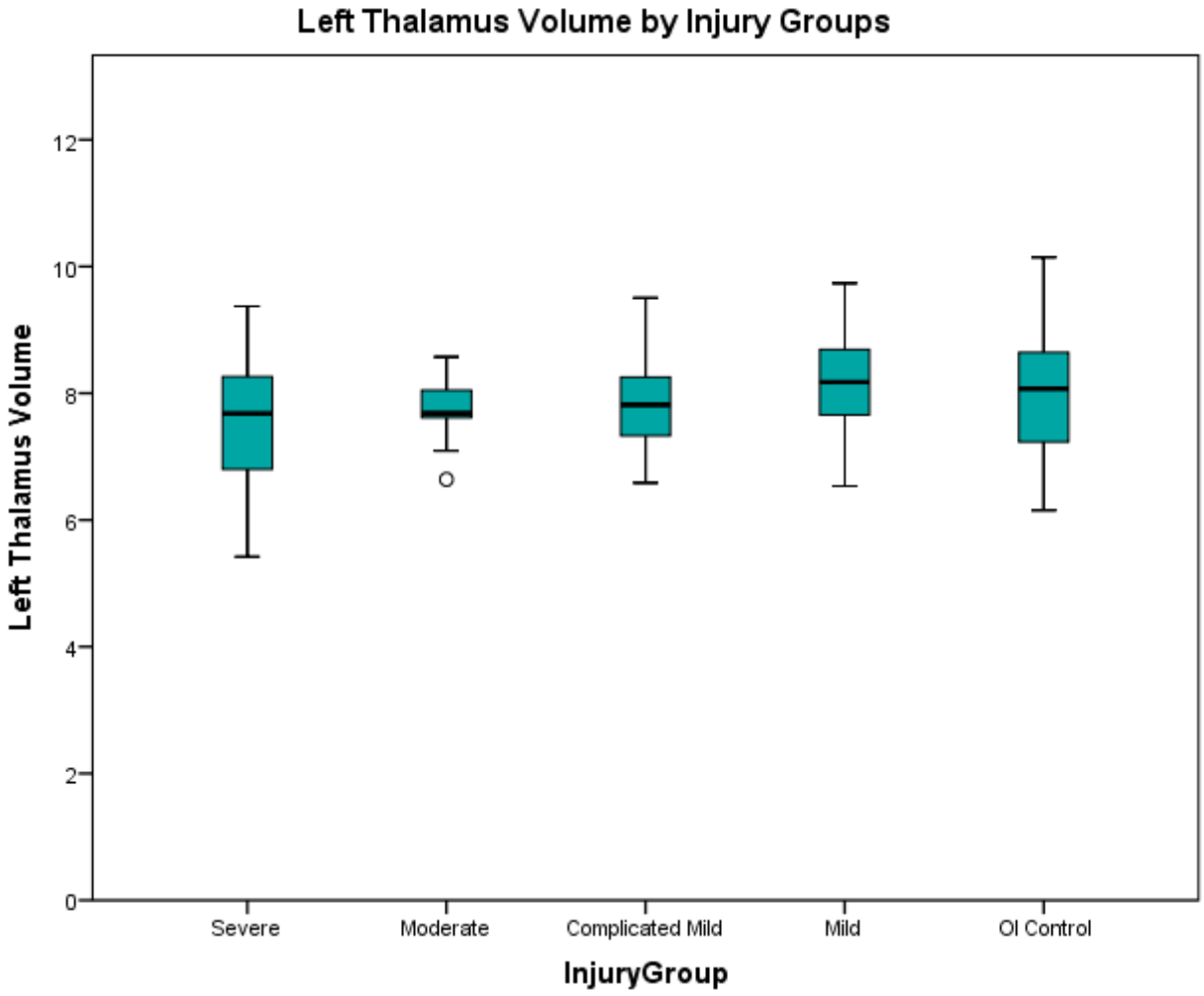

Figure 14: Left Thalamus Volume Means Between Subgroups. Boxplot showing between group differences for the left thalamus volume measurement. Volume measured in cm^3. Center line is group median and bars represent 95% confidence intervals. There were no significant differences between groups. Outliers represent data points greater than or equal to 1.5 standard deviations from mean for boxplot only.

Table 19: Adjusted and Unadjusted Measurement Means and Variability for Left Thalamus Volume Measurement with Brain Segmentation Volume and Age at Testing as Covariates

		Unadjusted		Adjusted	
	N	M	SD	M	SE
Severe	19	7.504	1.067	8.082	.133
Moderate	11	7.746	.557	7.893	.169
Complicated Mild	37	7.882	.694	7.977	.092
Mild	84	8.153	.680	7.971	.064
Control	97	8.034	.891	8.025	.057

Note: N = number of patients, M = Mean, SD = Standard deviation, SE = Standard error. All volumetric metrics are measured in millimeters (cm^3).

Table 20: Predicted Group Membership as Percentage Between Injury Groups

	Severe	Moderate	Complicated Mild	Mild	Control
Severe	47.4	36.8	10.5	0	5.3
Moderate	36.4	45.5	18.2	0	0
Complicated Mild	40.5	40.5	13.5	2.7	2.7
Mild	50.0	38.1	7.1	3.6	1.2
Control	39.2	49.5	6.2	1.0	4.1

Note: Control group is orthopedically injured patients. *10.5% percent of all cases classified correctly

Right Thalamus Measure

An ANCOVA was used for analysis. There was a linear relationship between right thalamus volume, and covariates, age at testing and brain segmentation volume, as assessed by visual inspection of a scatterplot. Homogeneity of regression slopes was confirmed as both interaction terms, ageattesting*injurygroup and brainsegvol*injurygroup, were not statistically significant, [F (4,233) = 1.579, p= .181, F (4,233) = .559, p= .693, respectively]. There was homogeneity of variances as assessed by Levene's test for homogeneity of variances (p= .203). Standardized residuals for individual groups and the overall model were normally distributed, as assessed by a Shapiro-Wilk test (p> .05). There were one outlier in the dataset as assessed by cases of standardized residuals greater than ±3 standard deviations. The ANCOVA was run with and without the outliers and statistically significant results remained unaffected. After adjustment of age at testing and brain segmentation volume there was no statistically significant difference

between the right thalamus volume measurement and injury groups, [F(4,241) = 1.938, p=.105, partial $\eta^2 = 0.031$; see Figure 15 and Table 21]. Prognostic power shown in Table 22.

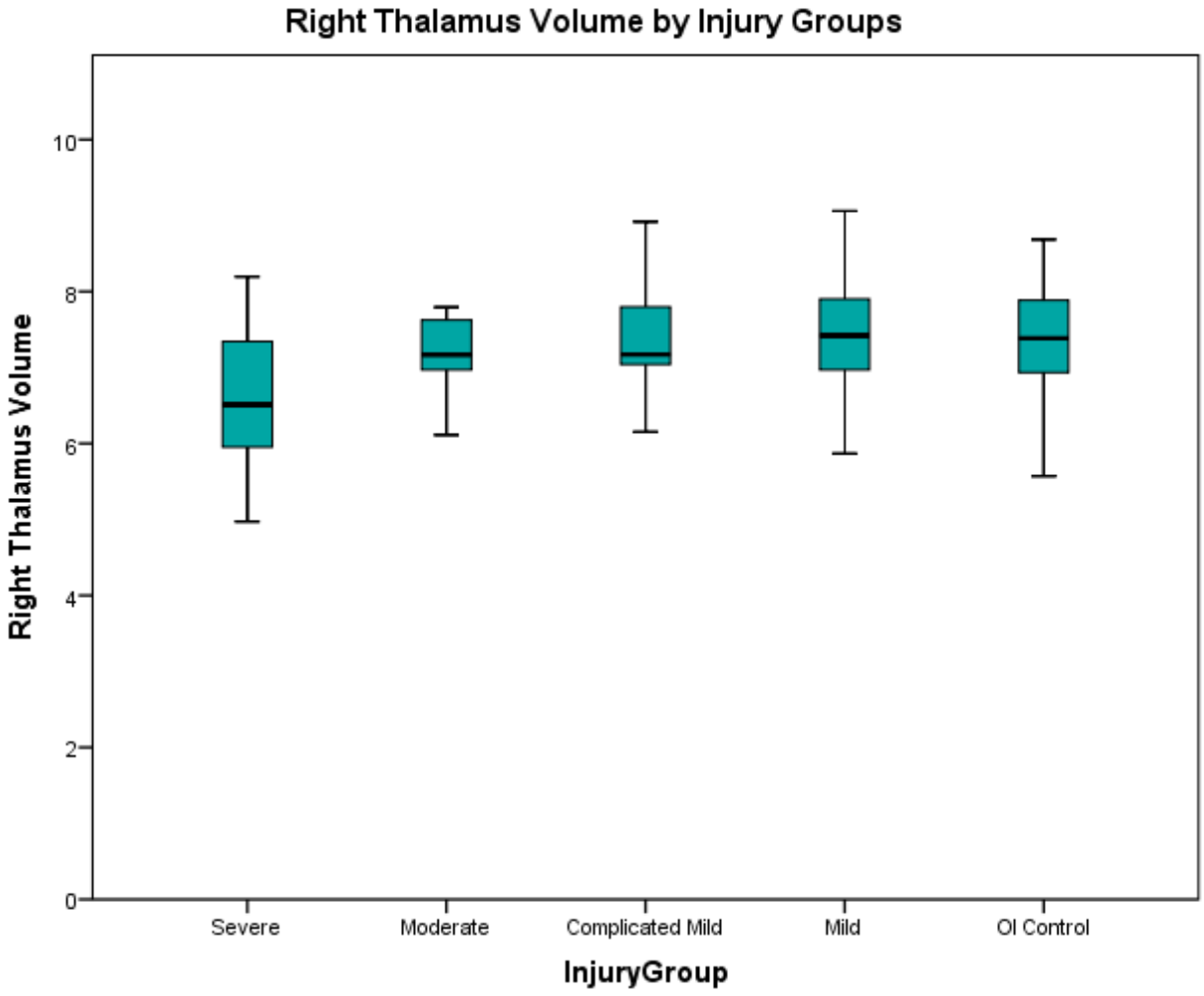

Figure 15: Right Thalamus Volume Means Between Subgroups. Boxplot showing between group differences for the right thalamus volume measurement. Volume measured in cm^3. Center line is group median and bars represent 95% confidence intervals. There were no significant differences between groups. Outliers represent data points greater than or equal to 1.5 standard deviations from mean for boxplot only.

Table 21: Adjusted and Unadjusted Measurement Means and Variability for Right Thalamus Volume Measurement with Brain Segmentation Volume and Age at Testing as Covariates

		Unadjusted		Adjusted	
	N	M	SD	M	SE
Severe	19	6.608	.912	7.074	.114
Moderate	11	7.181	.496	7.269	.145
Complicated Mild	37	7.387	.628	7.451	.079
Mild	84	7.472	.647	7.351	.056
Control	97	7.349	.702	7.328	.049

Note: N = number of patients, M = Mean, SD = Standard deviation, SE = Standard error. All volumetric metrics are measured in millimeters (cm^3).

Table 22: Predicted Group Membership as Percentage Between Injury Groups For Right Thalamus Measure

	Severe	Moderate	Complicated Mild	Mild	Control
Severe	47.4	5.3	36.8	5.3	5.3
Moderate	36.4	0	27.3	18.2	18.2
Complicated Mild	27.0	2.7	43.2	8.1	18.9
Mild	34.5	4.8	47.6	6.0	7.1
Control	37.1	4.1	40.2	10.3	8.2

Note: Control group is orthopedically injured patients. *15.3% percent of all cases classified correctly

Total Brain Segmentation Volume

An ANCOVA was used for analysis. There was a linear relationship between total brain segmentation volume, and covariates, age at testing and brain segmentation volume, as assessed by visual inspection of a scatterplot. Homogeneity of regression slopes was confirmed as the interaction term, ageattesting*injurygroup, was not statistically significant, [F (4,236) = .410, p= .795]. There was homogeneity of variances however, as evaluated Levene's test for homogeneity of variances (p= .793). Standardized residuals did notmeet the assumption of normality between all groups however as assessed with a Shapiro-Wilk test. Severe, moderate and complicated mild groups had p> .05 while the mild and control groups had p= .003, p= .008, respectively. The normality of standardized residuals for the overall model did not meet this assumption either, as assessed with a Shapiro-Wilk test, p= .001. Despite this, since ANCOVA is known to be fairly

robust against deviations from normality, it was the preferred statistical procedure. There were one outlier in the dataset as assessed by cases of standardized residuals greater than ±3 standard deviations. The ANCOVA was run with and without the outliers and statistically significant results remained unaffected. After adjustment of age at testing, there was a statistically significant difference between the total brain segmentation measurement and injury groups, [$F(4,241) = 3.521$, $p = .008$, partial $\eta^2 = 0.055$; see Figure 16 and Table 23]. Post-hoc analysis with a Bonferroni adjustment was performed. The severe TBI group was statistically significantly larger than the mild ($p = .010$) and control ($p = .005$) groups but not the moderate ($p = .421$) or complicated mild ($p = .092$). No other statistically significant results were seen. Prognostic power shown in Table 24.

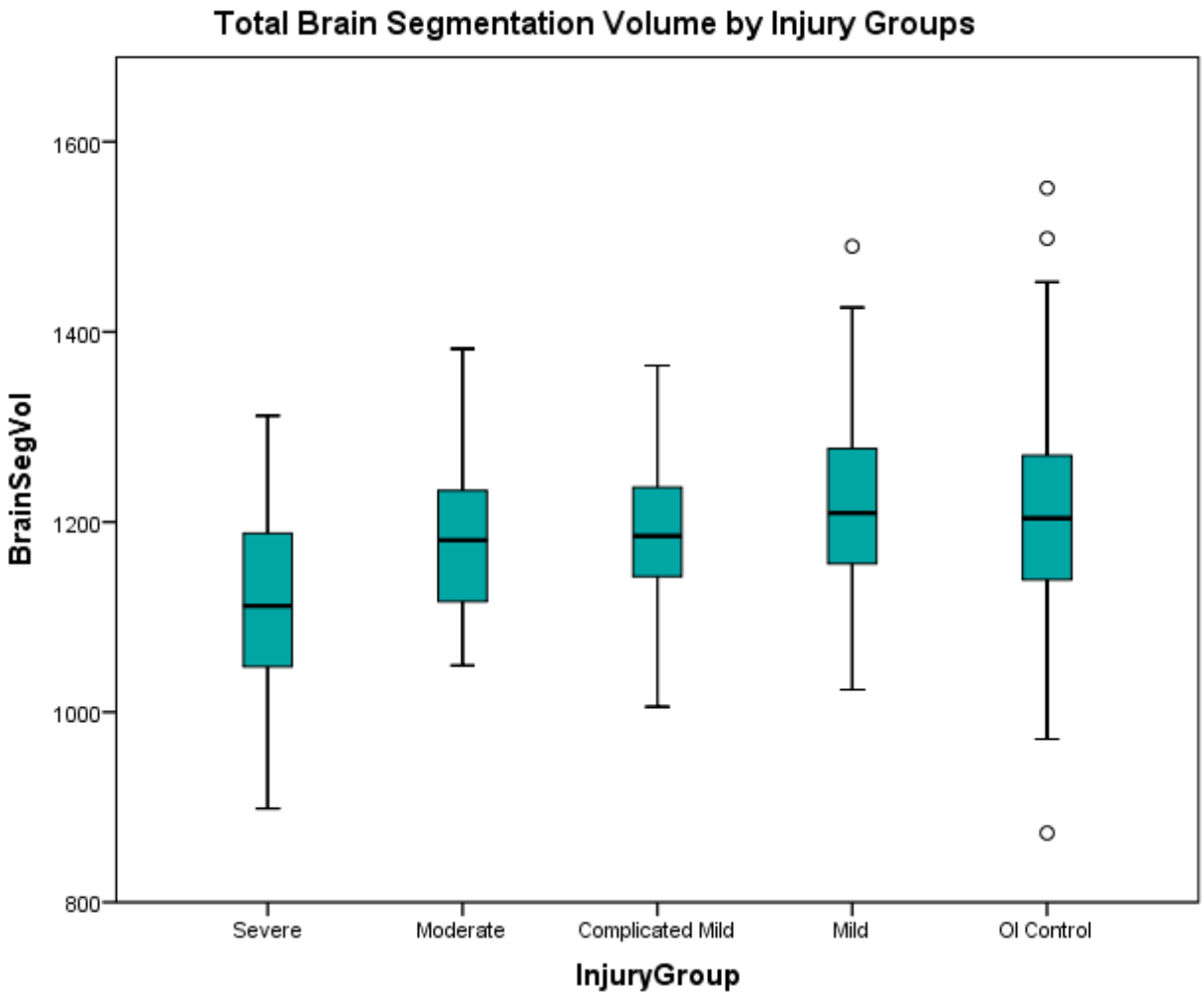

Figure 16: Total Brain Volume Means Between Subgroups. Boxplot showing between group differences for the total brain segmentation volume measurement. Volume measured in cm^3. Center line is group median and bars represent 95% confidence intervals. The severe TBI group was statistically significantly increased from the mild (p= .004) and control (p= .009) groups. Outliers represent data points greater than or equal to 1.5 standard deviations from mean for boxplot only.

Table 23: Adjusted and Unadjusted Measurement Means and Variability for Total Brain Segmentation Volume Measurement with Brain Segmentation Volume and Age at Testing as Covariates

		Unadjusted		Adjusted	
	N	M	SD	M	SE
Severe	19	1110.433	110.679	1126.755	22.153
Moderate	11	1192.803	103.253	1197.883	28.781
Complicated Mild	37	1192.901	84.662	1189.377	15.695
Mild	84	1218.403	102.995	1218.047	11.008
Control	97	1209.816	114.154	1207.696	9.696

Note: N = number of patients, M = Mean, SD = Standard deviation, SE = Standard error. All volumetric metrics are measured in millimeters (cm^3).

Table 24: Predicted Group Membership as Percentage Between Injury Groups For Total Brain Segmentation Volume

	Severe	Moderate	Complicated Mild	Mild	Control
Severe	57.9	15.8	5.3	15.8	5.3
Moderate	36.4	18.2	0	36.4	9.1
Complicated Mild	29.7	24.3	2.7	40.5	2.7
Mild	21.4	15.5	7.1	48.8	7.1
Control	29.9	13.4	4.1	42.3	10.3

Note: Control group is orthopedically injured patients. *26.2% percent of all cases classified correctly

CURRICULUM VITAE

51 East 600 North Provo, UT, 84606
(480) 720-0818 ▪ Email: csfinuf777@gmail.com

EDUCATION

2007-2013	B.S. - Neuroscience Brigham Young University-Utah, Provo, Utah
2014-Present	M.S. - Neuroscience Brigham Young University-Utah, Provo, Utah

RESEARCH ACTIVITIES

Pending Thesis

Finuf, C.S. (2016) *Third Ventricle Width as a Predictor of Brain Atrophy in Pediatric Traumatic Brain Injury.*

Published Abstracts

Bigler, E.D., Abildskov, T.J., Farrer, T.J., Finuf, C. S., Dennis, M., Taylor, H. G., Rubin, K. H., Gerhardt, C. A., Stancin, T. , Vannatta, K., Yeates, K. O. (2013) *Voxel-Based Morphometry of Gray and White Matter Correlates of WASI IQ and WISC-III Processing Speed Index in Pediatric Traumatic Brain Injury and Orthopedic Injury.* Journal of the International Neuropsychological Society, Volume 19, Supplement S1, pg. 122-123.

Z. McDonnell, Y.H. Tsui, C. Finuf, A. Hall, M. Gilmartin, J. Cummock, D. Skiles, D. Oleson, C. Hughes, D. Bjorn, M. Faulkner, S. Richardson, M. Killpack, E.D. Bigler, J.T. Tschanz, M.C. Norton & A. All Other Cache County Investigators. (2014) *Basal Ganglia Hyperintensities in Relation to the Modified Mini-Mental State (3MS) in the Cache County Study on Memory Health and Aging.* Journal of the International Neuropsychological Society, Volume 20, Supplement S1, pg. 154.

Y.H. Tsui, Z. McDonnell, C. Finuf, A. Hall, M. Gilmartin, J. Cummock, D. Skiles, D. Oleson, C. Hughes, D. Bjornn, M. Faulkner, S. Richardson, M. Killpack, E.D. Bigler, J.T. Tschanz, M.C. Norton & A. All Other Cache County Investigators. (2014) *Scheltens et al. Ratings For White Matter Hyperintensities in the Cache County Study on Memory Health and Aging.* Journal of the International Neuropsychological Society, Volume 20, Supplement S1, pg. 154-155.

Manuscripts Under Review

Bigler, E.D., Tsui-Caldwell, Y., McDonnell, Z., Christensen, Z., Finuf, C.S. (2014) *Scheltens Clinical Rating in the Cache County Memory in Aging Study.*

Manuscripts in Preparation

Finuf, C.S., McDonnell, Z., Faulkin, M., Tsui, Y., Skiles, D., Gilmartin, M., Richardson, S., Killpack, M., Hall, A., Hughes, C., Cummock, J., & Bigler, E.D. (2016). *Quantifying Brain Abnormalities in Alzheimer's Disease.*

Finuf, C.S., Christensen, Z., Hammond, T., Bigler, E.D. (2016) *Third Ventricle Width as a Predictor of Brain Atrophy in Pediatric Traumatic Brain Injury.*

Poster Presentations

Finuf, C.S., Hammond, T., Oleson, D., Tsui-Caldwell, Y., & Bigler, E.D. (2015). *Linear Third Ventricle Measurements as a Tool for Fast and Efficient Detection of TAI in Traumatic Brain Injury.* Presented at the Mary Lou Annual Conference at Brigham Young University, 2015.

Finuf, C.S., Song, X., Barr, C.S., Higley, J.D., Yang, Y. (2015). *Early-Life Stress Effects on Amygdala Volume and its Link to Anxiety-Like Behaviors.* Presented at National Institutes of Health Summer Poster Day in Bethesda, Maryland, 2015.

Finuf, C.S., Song, X., Barr, C.S., Higley, J.D., Yang, Y. (2015). *Early-Life Stress Effects on Amygdala Volume and its Link to Anxiety-Like Behaviors.* Presented at National Institute of Drug Abuse Summer Poster Day in Baltimore, Maryland, 2015.

Muncy, N., Doxey, C., Goodrich-Hunsaker, N., Finuf, C.S., South, M., Kirwan, B. (2014) *A Semi-Automated Algorithm for Segmenting the Hippocampus in Control and Patient Populations.* Presented at the 22nd Annual Meeting of the Cognitive Neuroscience Society, San Francisco, California, 2015.

Z. McDonnell, Y.H. Tsui, C. Finuf, A. Hall, M. Gilmartin, J. Cummock, D. Skiles, D. Oleson, C. Hughes, D. Bjorn, M. Faulkner, S. Richardson, M. Killpack, E.D. Bigler, J.T. Tschanz, M.C. Norton & A. All Other Cache County Investigators. (2014) *Basal Ganglia Hyperintensities in Relation to the Modified Mini-Mental State (3MS) in the Cache County Study on Memory Health and Aging.* Presented at the 42nd Annual Meeting of the International Neuropsychological Society, Seattle, Washington, 2014.

Y.H. Tsui, Z. McDonnell, C. Finuf, A. Hall, M. Gilmartin, J. Cummock, D. Skiles, D. Oleson, C. Hughes, D. Bjornn, M. Faulkner, S. Richardson, M. Killpack, E.D. Bigler, J.T. Tschanz, M.C. Norton & A. All Other Cache County Investigators. (2014) *Scheltens et al. Ratings For White Matter Hyperintensities in the Cache County Study on Memory Health and Aging.* Presented at the 42nd Annual Meeting of the International Neuropsychological Society, Seattle, Washington, 2014.

Finuf, C.S., McDonnell, Z., Faulkin, M., Tsui, Y., Skiles, D., Gilmartin, M., Richardson, S., Killpack, M., Hall, A., Hughes, C., Cummock, J., & Bigler, E.D. (2013). *Quantifying Brain Abnormalities in Alzheimer's Disease.* Presented at the Mary Lou Annual Conference at Brigham Young University, 2014.

PROFESSIONAL EXPERIENCE

Courses Assistant Taught-

Undergraduate Classes (Brigham Young University)

Physiology 362: Advanced Physiology- Dr. Dixon Woodbury

Physiology 362: Advanced Physiology- Dr. Dave Kooyman

Physiology 362: Advanced Physiology- Dr. James Porter

Psychology 492R: Superv Instrctnl/Resrch Exper- Dr. Erin Bigler

Psychology 712R: Topics in Neuropsychology- Dr. Erin Bigler

August 2011 – 2013

Research Assistant, Brain Imaging & Behavior Lab.

- Working as an undergraduate research assistant in various areas of neuropsychology and neuropathology. Supervisor: Erin D. Bigler, Ph.D., Brigham Young University.

January 2014- Present

Research Assistant, Brain Imaging & Behavior Lab.

- Working as a graduate research assistant with traumatic brain injury patients. Supervisor: Erin D. Bigler, Ph.D., Brigham Young University.

May 2014- Present

Research Assistant, Primate Research Lab

- Data analyst. Supervisor: J. Dee Higley, Ph.D., Brigham Young University.

June 2015-August 2015

Summer Intern, National Institute of Drug Abuse

- Lead on a project which focused on early-life stressors and its link to anxiety-like behaviors. Supervisor: Yihong Yang, Ph.D., University of Illinois at Urbana-Champaign, Urbana.